THE ROLE OF THE E3-UBIQUITIN LIGASE TRIM17 IN THE MITOCHONDRIAL CELL DEATH PATHWAY

BY

JENNIFER E. CRICHTON

Thesis submitted to the School of Graduate and Post-doctoral studies,
University of Ottawa, in partial fulfillment of the requirements for the degree of
Master of Science

Department of Biochemistry, Microbiology and Immunology,
Faculty of Medicine, University of Ottawa

Abstract

The upregulation of apoptosis is a hallmark of several neurodegenerative disorders including ischemic stroke. In neurons, as in other cell types, Bax and tBid are critical regulators of the intrinsic pathway upstream of mitochondrial outer membrane permeabilization (MOMP) and caspase activation. The characterization of the molecular events that occur during the early stages is therefore extremely important from a therapeutic standpoint. Here I show that two independent genetic pilot screens looking for novel regulators of Bax activation identified a common hit in the E3 ubiquitin ligase Trim17. Knockdown of Trim17 was found to protect against tBid-induced death in primary cortical neurons and allowed for the maintenance of mitochondrial function and oxidative phosphorylation under this apoptotic stress. The RING-domain of Trim17 was found to interact with Opa1 in mouse brain extracts. Furthermore, Opa1 co-immunoprecipitated with exogenously expressed full-length Trim17 from HEK293 cells. Knockdown of Trim17 in neurons increased Opa1 protein levels under steady-state conditions. These results suggest that Trim17 regulates Bax-dependent apoptosis in neurons via the modulation of Opa1 levels.

Acknowledgements

First and foremost I would like to acknowledge my supervisor Dr. Robert Screaton and express my gratitude for his encouragement, guidance, and humour. I would to express my gratitude to Dr. Stephen Baird for his technical expertise and endless patience, Darcey Miller for her guidance during the early stages of this project, and the rest of the Screaton lab for their endless support and continual supply of comedic relief. I would also like to thank my Thesis Advisory Committee – Dr. Douglas Gray and Dr. Steffany Bennett for their direction and input. I am also grateful for all of the staff and researchers at the Apoptosis Research Centre, in particular Lynn Kelly and Kathleen Frost who play a huge part in allowing us to focus our energies on the research side of things.

Table of Contents

List of Abbreviations……..vi

List of Figures……...viii

List of Appendices……ix

Chapter 1: Introduction……..1

1.1 Apoptosis……1
1.2 Intrinsic pathway of apoptosis……2
1.3 Bcl-2 proteins and the regulation of the intrinsic pathway……..9
1.4 Mitochondrial dynamics and the regulation of apoptosis……..13
1.5 Ubiquitin-mediated regulation of apoptosis……19
1.6 Trim proteins and their roles as E3 ubiquitin ligases……..21
1.7 Neuronal apoptosis in neurodegeneration……..24
1.8 Hypothesis and objectives……28

Chapter 2: Materials and Methods……29

2.1 Genetic screens to identify novel regulators of Bax activation……....29
2.2 Generation of shRNA-expressing lentivirus…….....30
2.3 Cell culture of mouse embryonic cortical neurons…….....31
2.4 Assay for cell death in cortical neurons…….....31
2.5 TMRE and ATP measurements in cortical neurons…….....32
2.6 OCR measurements in cortical neurons…….....32
2.7 Proteomic screen I: HEK293 Flp-In TRex cells…….....33
2.8 Proteomic screen II: GST-RING-TRIM17 in mouse brain extracts…..34
2.9 FLAG-immunoprecipitation from HEK293 Flp-In TRex cells…….....35
2.10 Subcellular fractionation of cortical neurons…….....35

Chapter 3: Results……38

3.1 Pilot screens for regulators of Bax activation…….....38
3.2 Knockdown of Trim17 delays cell death in cortical neurons……....38
3.3 Mitochondrial function is maintained after tBid in Trim17 knockdown neuronal cultures.…….....44
3.4 Identification of Trim17 protein-complex members…….....48
3.5 Trim17 forms a complex with Opa1 and facilitates its degradation.....54

Chapter 4: Discussion…….....58

Conclusion…….....67

References…….....68

Contribution of Collaborators…….....79

Appendices…….....80

Curriculum Vitae…….....86

List of Abbreviations

$\Delta\Psi$	mitochondrial membrane potential
Ad-tBid	adenovirus overexpressing HA-tBid
Ara-c	cytosine β-D-arabinofuranoside, mitotic inhibitor
BCA	bicinchoninic acid
Bcl-2	b-cell lymphoma, family of pro- and anti-apoptotic proteins, also the name of a single anti-apoptoic family member
Bid	pro-apoptotic member of the Bcl-2 family, BH3-only protein
CGNs	cerebellar granule neurons
CHAPS	3-[(3-Colamidopropyl)dimethylammonio]-1-propanesulfonate, non-ionic detergent
DIV	day in vitro
ETC	electron transport chain
FCCP	trifluorocarbonylcyanide phenylhydrazone
FCS	fetal calf serum
GST	glutathione S-transferase
HA	hemagglutinin
IP	immunoprecipitation
IF	immunofluorescence
IMM	inner mitochondrial membrane
Lancl-1	LanC lantibiotic synthetase component C-like 1
Mcl-1	myeloid cell leukemia-1, anti-apoptotic Bcl-2 family member
MS	mass spectrometry
MOMP	mitochondrial outer membrane permeabilization

NSF	N-ethylmaleimide sensitive fusion protein
OCR	oxygen consumption rate
OGD	oxygen-glucose deprivation
OMM	outer mitochondrial membrane
OPA1	optic atrophy 1
PBS	phosphate-buffered saline
PVDF	polyvinylidene fluoride
QVD	Q-VD-OPh, chemical pan-caspase inhibitor
RING	really interesting new gene
RLU	relative light units
SDS-PAGE	sodium dodecyl sulfate polyacrylamide gel electrophoresis
shRNA	short hairpin RNA/ribonucleic acid
SN	supernatant
tBid	truncated or activated Bid
TBS	Tris-buffered saline
TBS-T	Tris-buffered saline supplemented with 1% Tween
Tet	tetracycline
TMRE	tetramethylrhodamine
TRIM17	tripartite motif 17 (gene name)
TX100	Triton X-100
WB	Western blot

List of figures

1. Extrinsic and intrinsic pathways of apoptosis.

2. Mitochondrial dynamics and the regulation of apoptosis.

3. Two independent pilot genetic screens identify TRIM17 as being required for Bax activation

4. Loss of TRIM17 delays cell death in cortical neurons.

5. Mitochondrial function is maintained in the presence of tBID in cortical neurons lacking TRIM17.

6. Proteomic screen (I) to identify interacting partners of TRIM17.

7. Proteomic screen (II) to identify interacting partners of the RING domain of TRIM17.

8. TRIM17 forms a complex with and regulates OPA1.

9. Proposed model for the biological effect of an OPA1-TRIM17 complex.

List of Appendices

A. Verification of Hoechst toxicity in live cortical neurons for nuclear morphology assay.

B. Mass spectrometry data for the top 98 hits from the HEK293 Flp-In Trex proteomic (I) screen.

C. Proteomic screen (II) to identify interacting partners of the RING domain of TRIM17.

D. Mass spectrometry data for bands 1 (~90kDa), 2 (~74kDa) and 4 (~40kDa) from pulldown with GST-RING-TRIM17 in mouse brain extracts.

E. The RING domain of TRIM17 forms a complex with NSF and both alpha- and beta-tubulin in mouse brain extracts.

Chapter 1: Introduction

1.1 Apoptosis

Apoptosis is a tightly controlled process that is critical for both the normal development and maintenance of tissues. It can be triggered by a variety of physiological and pathological environmental stimuli. It is often termed programmed cell death because it proceeds by a controlled sequence of events and is marked by several morphological features that include blebbing, loss of cell attachment, nuclear condensation and chromosomal DNA fragmentation [1]. Changes in cell surface proteins on apoptotic cells permit their elimination through phagocytosis by neighbouring cells and macrophages [2]. Apoptosis differs from necrosis, the other commonly referred to form of cell death, in that it is an active, controlled process of cellular dismantling that prevents the release of inflammatory molecules into the extracellular environment and tissues [3].

The apoptotic program is triggered and amplified by two distinct pathways. The extrinsic, or immune-mediated, pathway involves the binding of a pro-apoptotic ligand to an extracellular death receptor [4]. The intrinsic, or mitochondrial, pathway is governed by the integration of numerous signaling cascades by mitochondria. This pathway is triggered through developmental cues or cellular stresses such as endoplasmic reticulum (ER) stress, changes in electron transport, loss of mitochondrial membrane potential ($\Delta\Psi$), changes in the levels of Bcl-2 family proteins, calcium (Ca^{2+}) overload or DNA damage [5]. Regardless of the initiation phase of apoptosis, the end result is the activation and cleavage of the cysteine-

aspartic (caspase) family of proteases [6]. The conversion of caspases from their inactive pro-form to their proteolytically-active form can be subdivided into two types. Auto-activation of the initiator caspases (e.g. Casp 2, 8, 9, 10) occurs first and is required for the cleavage and activation of the executioner caspases (e.g. Casp 3, 6, 7). These downstream executioner caspases continue the apoptotic cascade by cleaving other protein substrates, ultimately leading to DNA fragmentation and cell death [7]. Cross talk between the extrinsic pathway and the intrinsic pathway can occur in some cell types and is mediated by the proteolytic cleavage of Bid (discussed further below) by caspase 8 [8].

Aberrant apoptosis can give rise to a number of human disorders. The upregulation of apoptosis is a hallmark of several disease states such as stroke, diabetes, and Alzheimer's and Parkinson's diseases [9, 10]. These conditions have unique disease etiologies but share a common biochemical cascade of events that appear to carry out the associated cell death. This process includes the disruption of cellular calcium homeostasis, increased oxidative stress and activation of apoptosis [10]. On the other hand, a lack of timely cell death underlies many forms of cancer [11]. The complete understanding of apoptosis is therefore crucial in a variety of disease contexts.

1.2 Intrinsic pathway of apoptosis

Activation of the intrinsic pathway of apoptosis results in a series of signaling events that converge on mitochondria. Mitochondrial outer membrane permeabilization (MOMP) is an early event in this pathway that is associated with

the collapse of mitochondrial membrane potential, the loss of oxidative phosphorylation (ATP synthesis) and the release of pro-apoptotic proteins from within the mitochondrial inner membrane space (IMS) [12]. This release of pro-death factors precedes caspase activation. In particular, the release of cytochrome *c* from the IMS is a key event that is followed by its binding to apoptotic protease activating factor 1 (Apaf1) in the cytosol [13, 14]. This binding induces the conformational change and oligomerization of Apaf1 and in turn, guides the formation of a multimeric protein complex, termed the apoptosome, in an ATP-dependent fashion [15]. The apoptosome is then able to activate caspase 9, which goes on to cleave and activate the executioner caspases. The parallel release of second mitochondrial-derived activator of caspase (SMAC) and OMI (also known as Htr A serine peptidase-2 or HTRA2) from mitochondria serve to maintain caspase activity during this time by blocking the activity of the inhibitor of apoptosis proteins (IAPs) (Figure 1) [16].

In addition to the above-mentioned proteins, the release of two other factors from mitochondria serves to promote caspase-independent death. Endonuclease G, once released from mitochondria, translocates to the nucleus and cleaves chromosomal DNA into small nucleosomal fragments [17]. Apoptosis inducing factor (AIF) is another protein that, when released from mitochondria, translocates to the nucleus, binds DNA and promotes chromatin condensation independently of caspases (Figure 1) [18]. Upon activation of these downstream caspases and nucleases the cell begins to assume an apoptotic morphology.

The B-cell lymphoma (Bcl-2) family of proteins contains the key regulators of

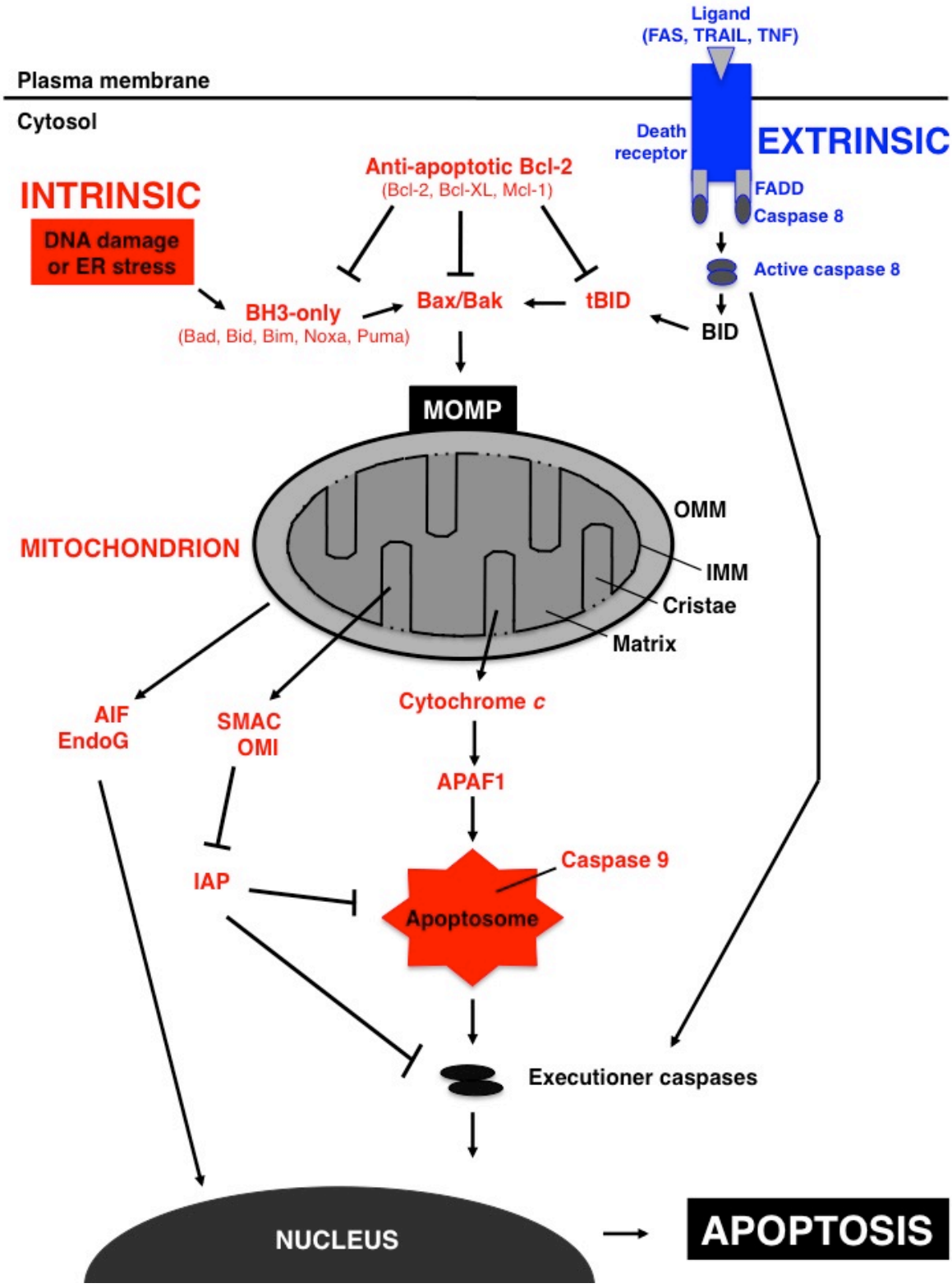
Ligand
(FAS, TRAIL, TNF)
Plasma membrane
Cytosol
Death
receptor
EXTRINSIC
FADD
Caspase 8
Active caspase 8
INTRINSIC
DNA damage
or ER stress
Anti-apoptotic Bcl-2
(Bcl-2, Bcl-XL, Mcl-1)
BH3-only
(Bad, Bid, Bim, Noxa, Puma)
Bax/Bak
tBID
BID
MOMP
MITOCHONDRION
OMM
IMM
Cristae
Matrix
AIF
EndoG
SMAC
OMI
Cytochrome c
APAF1
IAP
Caspase 9
Apoptosome
Executioner caspases
NUCLEUS
APOPTOSIS

Figure 1. Extrinsic and intrinsic pathways of apoptosis. The extrinsic pathway is stimulated by the binding of ligands to death receptors. The subsequent dimerization and activation of caspase 8 leads to the activation of downstream executioner caspases (3 & 7) that carry out the remainder of the cell death program. The intrinsic pathway is initiated by various stimuli, such as DNA damage or endoplasmic reticulum (ER) stress. This activates the pro-apoptotic BH3-only and the subsequent activation of Bax and Bak. Anti-apoptotic Bcl-2 family members oppose Bax/Bak activation via binding to directly or indirectly by binding BH3-only proteins. Activation of Bax/Bak triggers their oligomerization on the outer mitochondrial membrane (OMM) that leads to mitochondrial outer membrane permeabilization (MOMP). MOMP gives rise to the release of numerous apoptogenic factors from within mitochondria. Released cytochrome c binds Apaf1 in the cytosol, allowing for the formation of the apoptosome that recruits and activates the initiator caspase 9. Downstream executioner caspases are then activated by caspase 9 and go on to carry out the later stages of the apoptotic program. The release of pro-apoptotic Smac and Omi serve to maintain caspase activity through the inhibition of IAPs. Additionally, the release of AIF and EndoG promotes a caspase-independent form of the intrinsic pathway. These factors translocate to the nucleus and trigger chromatin condensation and DNA fragmentation. Cross-talk between the extrinsic and intrinsic pathways may occur through the activation of Bid to tBid in some cell types, under some conditions. Common elements to both pathways are shown in black, elements specific to the extrinsic pathway are shown in blue, elements specific to the intrinsic pathway are shown in red.

this pathway upstream of MOMP. Members of the Bcl-2 family are subdivided by the number (one or more) of the four characteristic Bcl-2 homology (BH) domains that they possess. BH domains are crucial for their either pro- or anti-apoptotic function. The cytosolic Bcl-2 associated X protein (Bax) and the mitochondrial Bcl-2 antagonist or killer (Bak) are two pro-apoptotic members that must be activated for MOMP to occur. Cells deficient in both Bax and Bak, but not singly-deficient cells, have been shown to be resistant to cytochrome *c* release and cell death [19]. Both Bax and Bak can be activated during apoptosis by the caspase 8 cleaved-form of the pro-apoptotic, BH3-only protein Bid (truncated Bid, or tBid) [20-22]. Once activated, Bax and Bak undergo a range of conformational changes as well as the translocation of Bax from the cytosol to the outer mitochondrial membrane (OMM) [22]. With its conformational change Bax reveals an epitope in its N-terminus, normally hidden, that becomes recognizable by the 6A7-antibody [23-25]. Studies in Bax/Bak-deficient mouse embryonic fibroblasts (MEFs), in which Bax has been reconstituted with an oligomerization-deficient mutant, have shown that these cells are still unable to undergo apoptosis despite the exogenous expression of this mutant Bax [26]. With similar findings having been shown for Bak [27], the homo-oligomerization of these two proteins on the OMM is therefore most likely required for MOMP.

In addition to homo-oligomerization being necessary for MOMP, there is evidence for a direct interaction between tBid and Bax. With fluorescence techniques and an *in vitro* system, it has been shown that tBid rapidly binds to membranes, where it interacts directly with Bax. This results in facilitated Bax

insertion and homo-oligomerization in membranes [28]. Furthermore, it has recently been suggested that the mitochondrial carrier homolog-2 (Mtch2), a surface-exposed OMM protein, is a critical facilitator of tBid recruitment to mitochondria. Embryonic stem cells and MEFs lacking Mtch2 showed a reduction in mitochondrial-tBid, activated Bax/Bak, MOMP and apoptosis in response to a death stimulus [29]. These data suggest that there are a number of factors involved in the activation of Bax/Bak prior to MOMP and therefore there also exists the potential for the identification of novel regulators of this process.

The means by which pro-apoptotic factors are released from within mitochondria following MOMP has been proposed to occur by various, and often conflicting, mechanisms. Early studies described the formation of a mitochondrial permeability transition pore (MPTP) during apoptosis. The MPTP is proposed to have several protein members. Some of the identified complex members include the voltage-dependent anion channel (VDAC) on the OMM, the adenine nucleotide translocator (ANT) on the inner mitochondrial membrane (IMM) and cyclophilin D (Cyp D) in the mitochondrial matrix (MM) [30, 31]. This protein complex allows for the influx of water into the MM, causing osmotic swelling, the rupture of both the IMM and the OMM and finally the release of mitochondrial proteins into the cytosol. The dispensability of the MPTP itself as well as the necessity of all of the individual complex members for MOMP has been debated [32, 33]. Accordingly, it has been shown that mitochondria from Cyp D-deficient mice are resistant to normal MOMP inducers such as excess Ca^{2+} and reactive oxygen species (ROS), but are readily permeabilized by Bax and tBid [34, 35]. Another model suggested that a large pore

formed by VDAC, the major permeability pathway for metabolites in the OMM, and Bax was responsible for the release of cytochrome *c* from the IMS [36-38]. This finding was later refuted by *in vitro* work showing no detectable interaction between VDAC and Bax, therefore eliminating the possibility that Bax induces cytochrome *c* release by acting on VDAC. However, it was found that tBid induced VDAC-closure, perhaps contributing to mitochondrial dysfunction through limited metabolite exchange between mitochondria and the cytosol [39]. VDAC has now been completely ruled out for a role in permeability transition as loss of all three isoforms does not affect apoptotic sensitivity [40].

An alternative mechanism by which mitochondrial proteins may leak out into the cytosol is through the formation of proteinaceous pores. Bax and Bak oligomers are capable of forming pores in the OMM that allow for the release of pro-apoptotic proteins into the cytosol [41, 42]. This was first hypothesized because of the structural similarities between Bax and known bacterial pore-forming toxins [43]. Building on this alternative model, is the idea that the interaction of OMM lipids with Bax/Bak oligomers causes membrane bending and the subsequent formation of transient lipid pores. These pores take on an inverted micelle structure and would thereby allow the release of mitochondrial contents [44, 45]. The possibility that these different modes of MOMP may cooperate at the same time or in sequence is a topic that is now being explored.

1.3 Bcl-2 proteins and the regulation of the intrinsic pathway

The initiation of MOMP is generally considered to be a point of no return within the intrinsic pathway. As mentioned above, the Bcl-2 family of proteins is largely responsible for the regulation of MOMP. This family can be subdivided based on their BH domain organization. The pro-apoptotic members are classed as the effectors (Bax, Bak and Bok) that directly cause MOMP or the BH3-only (tBid, Bim, Bad, Bik, Bmf, Bnip3, Hrk, Noxa and Puma) that relay the apoptotic signal to the effectors. The pro-survival members represent a single class and contain all four BH domains (Bcl-2, Bcl-W, Bcl-XL, A1A and Mcl-1) [16].

The transcriptional regulation of Bcl-2 proteins is a means by which cells control the initiation of apoptosis. This regulation varies depending on the family member. The expression of some BH3-only proteins can be induced by transcription factors. For example, the tumor suppressor p53 induces Noxa and Puma in response to DNA damage [46], whereas the class O forkhead box transcription factor-3A (FOXO3A) induces Bim as a result of growth-factor deprivation [47]. In addition to regulating Noxa and Puma, p53 also induces Bid and Bax transcription and can negatively regulate the expression of Bcl-2 [48, 49]. Conversely, transcription of the anti-apoptotic Bcl-XL protein can be induced by the Janus kinase-signal transducer and activator of transcription (JAK-STAT) pathway to promote cell survival [50]. While p53 does play a role in the transcription of Bax, it is important to note that Bax appears to be constitutively expressed at relatively constant levels. It is therefore the post-translational regulation of Bax that is the main factor in determining its activity [51].

The means by which the Bcl-2 proteins regulate MOMP is an area of controversy. At a basic level, it is known that this family of proteins can form either homo- or heterodimers to dictate mitochondrial integrity but the exact nature of these dimers is a topic of debate [52]. Two models currently exist: the indirect activator model and the direct activator model. The indirect model predicts that Bax and Bak remain bound in an active state by anti-apoptotic Bcl-2 proteins. It is the competitive interaction of BH3-only proteins with the anti-apoptotic family members that permits the release of activated Bax and Bak [53, 54]. The direct model asserts that the interaction of Bax or Bak with a subset of BH3-only proteins (known as direct-activators) triggers their activation. This model argues that anti-apoptotic Bcl-2 proteins prevent MOMP either by sequestering these BH3-only proteins or binding directly to, and inhibiting, active Bax/Bak [55-57]. Consistent with the direct activator model and in the case of Bax activation, the use of full-length recombinant proteins and liposomes *in vitro* has shown that Bcl-XL is capable of binding directly to both tBid as well as active and inactive Bax. All of these forms of binding were found to decrease Bax oligomerization and liposome permeabilization [58]. Bcl-XL therefore likely functions as a dominant-negative, oligomerization-deficient Bax. Within the direct-activator model, there exists a subset of BH3-only proteins that are termed sensitizers as they cannot directly activate Bax/Bak but serve to neutralize anti-apoptotic Bcl-2 proteins [16]. In any case, the debate over these models continues, with the possibility of both holding true in different scenarios [59-62]. The most important determinant in the decision to initiate apoptosis may lie in the stoichiometric ratios of anti- versus pro-apoptotic Bcl-2 family members. For the

purposes of the present study, I will focus here on the different mechanisms by which Bax activation is currently known to occur.

The necessity of Bax to cause MOMP and activation of the caspase cascade is undisputed. Various developmental cues and cytotoxic agents can activate Bax, however, the precise molecular mechanism by which this occurs is not currently known. Bax consists of nine alpha helices and exists primarily in two stable conformations: native Bax that is present in the cytosol and fully activated Bax that inserts into the OMM. Studies employing cell-free mitochondria and liposome permeabilization to measure Bcl-2 protein interactions have been successful in providing robust evidence for the interaction of several BH3-only proteins with some family members [57, 63]. However, these same approaches have given weak evidence for the binding of full-length Bid, tBid or Bim to Bax [54]. Modified versions of BH3-only proteins termed stabilized alpha-helix of Bcl-2 domains (SAHBs), including those for Bid and Bim, have been shown to bind to Bax at an interaction site that is unique from the canonical binding groove characterized for the anti-apoptotic proteins [64, 65].

More recent *in vivo* work argues for the critical role of Bid, Bim and Puma in Bax activation. By using Bid/Bim/Puma triple knockout (KO) mice, the authors show that deletion of these genes causes an impaired apoptotic response. In neurons from these triple KO mice it was observed that Bax/Bak homo-oligomerization, cytochrome c release and caspase activation was prevented in response to numerous death stimuli [66]. Another recent study from this group characterizes the molecular mechanism of Bax insertion into the OMM. The authors describe the

stepwise structural reorganization that leads to its homo-oligomerization on the OMM. In its cytosolic form, the α9 helix of Bax is maintained in the "dimerization pocket" by the α1 helix. The α1 helix becomes exposed as a result of activator BH3-only proteins, such as tBid, and releases the α9 helix allowing for its insertion into the OMM. Furthermore, homo-oligomerization is promoted through the continued interaction of tBid with the N-terminal BH1 domain of Bax [67]. These data therefore provide additional evidence for the direct activator model and point to an important role for tBid in Bax activation.

The elucidation of the mechanism of Bax activation has proven challenging. Given what is currently known about this process, there are several points at which regulation could theoretically occur via non-Bcl-2 proteins. Contact sites between the endoplasmic reticulum (ER) and mitochondria are mediated by the OMM protein mitofusin-2 (Mfn2) [68]. These sites allow for the transfer of calcium and lipids between these organelles, but can also influence the spread of cellular signaling cascades, such as those that occur during apoptosis. The possibility of an ER membrane-influence on Bax activation was recently explored. The sphingolipid hexadecenal, synthesized through the conversion of ceramide by ER sphingomyelinases, was found to greatly enhance Bax oligomerization in purified mitochondria [69]. These results provide further insight into the nature of the OMM environment required for Bax activation. In addition, the regulation of Bax levels via the ubiquitin-proteasome system has been proposed as another means to regulate apoptosis. The anti-apoptotic effects of the E3-ubiquitin ligase Parkin, most well

known for its requirement in a form of mitochondrial quality control (mitophagy), are proposed to occur via its direct ubiquitination of Bax. Overexpression of Parkin prevents Bax translocation to mitochondria under apoptotic conditions. Futhermore, the anti-apoptotic effect of Parkin overexpression was abolished in Bax KO cells complemented with a ubiquitination-resistant mutant Bax [70]. These data provide rationale for the existence of additional, non-Bcl-2 family regulators of Bax activation and MOMP.

1.4 Mitochondrial dynamics and the regulation of apoptosis

During apoptosis a variety of cellular signals converge on mitochondria. As outlined in previous sections, these dynamic organelles play a critical role in the cell's commitment to death. In addition to being a milieu for the propagation of cellular signals, mitochondria have been found to undergo extensive morphological changes during apoptosis. Under steady-state conditions, mitochondria exist in a network of tubular-like structures. These structures undergo continuous fission and fusion events that are controlled largely by the dynamin-related proteins [71]. In humans, the fission machinery is composed of dynamin-related protein-1 (Drp1), fission 1 (Fis1) and Rab32 (member of the ras oncogene family). Drp1 and Rab32 are GTPases whose catalytic activity is required for membrane fission, whereas Fis1 is believed to aid in Drp1 recruitment to fission sites [72]. On the other end, the most well known components of the fusion machinery are three different dynamin-related proteins with GTPase activity: optic atrophy-1 (Opa1) and mitofusins 1 and 2

(Mfn1, Mfn2). Together, these proteins serve to mediate fusion of both the IMM and OMM [73].

The modulation of mitochondrial dynamics during apoptosis is a widely accepted phenomenon, however a cause versus effect role for the fission and fusion machinery has been a topic of debate. An increase in fission and subsequent fragmentation of the mitochondrial network is closely associated with apoptosis triggered by a variety of stimuli [74, 75]. Cytosolic Drp1 is recruited early on during apoptosis and has been shown to colocalize at fission sites with Bax and Mfn2 [76]. The identification of Mfn2 as an ER-mitochondria tethering protein and the more recent evidence implicating the ER-secreted sphingolipid hexedecenal in the facilitation of Bax activation suggest these inter-membrane contact sites may be important for the initiation of MOMP [68, 69]. Conversely, the inactive, soluble form of Bax has been shown to positively regulate mitochondrial fusion through Mfn2 homo-complexes under steady-state conditions [77]. The translocation of Bax from the cytosol to the OMM may represent a means by which the cell can slow the rate of fusion and shift the equilibrium towards a more fragmented state during apoptosis. In contrast to this, the stabilization of active Bax on the OMM, despite the overexpression of the antagonistic Bcl-XL blocking oligomerization and cytochrome *c* release, appears to be sufficient to trigger fission [78]. Thus it appears that mitochondrial fragmentation during apoptosis does not absolutely require MOMP. It therefore appears as if Bax differentially regulates mitochondrial dynamics depending on its conformation.

Genetic manipulation of the fission and fusion machinery has been a valuable tool in investigating the relationship between mitochondrial morphology and cell survival. It is generally thought that inhibition of the fusion machinery gives rise to a more fragmented mitochondrial network that is sensitized to apoptotic stimuli (Figure 2). On the other hand, inhibition of the fission machinery causes elongation of the network and usually confers protection against apoptotic stimuli [79, 80]. This was shown using RNA interference to knockdown Fis1, Drp1, and Opa1 in Hela cells. Fis1 knockdown was found to provide an even greater protection against actinomycin D-induced cytochrome *c* release compared to Drp1 knockdown. It was also found that down-regulation of Fis1 additionally blocked Bax activation, whereas loss of Drp1 had no effect. In the other direction, Opa1 knockdown cells were severely sensitized to the apoptotic stimulus, with a portion of the cells undergoing spontaneous death that was found to require Fis1 expression [81]. This landmark study showed that fragmentation of the mitochondrial network alone does not result in apoptosis but instead provided strong evidence for the role of the fission and fusion machinery in the regulation of cell fate. For the purposes of the current work, the specific role of Opa1 in the remodeling of the IMM and cytochrome c release following MOMP is discussed in detail in the next section.

MOMP causes extensive remodeling of mitochondrial ultrastructure in addition to the fragmentation of the network across the cell. These additional changes occur primarily at the involutions of the IMM known as cristae. The point at which the IMM of two individual cristae meet is termed the cristae junction. Under steady-state conditions, cristae serve to increase the surface area of the IMM

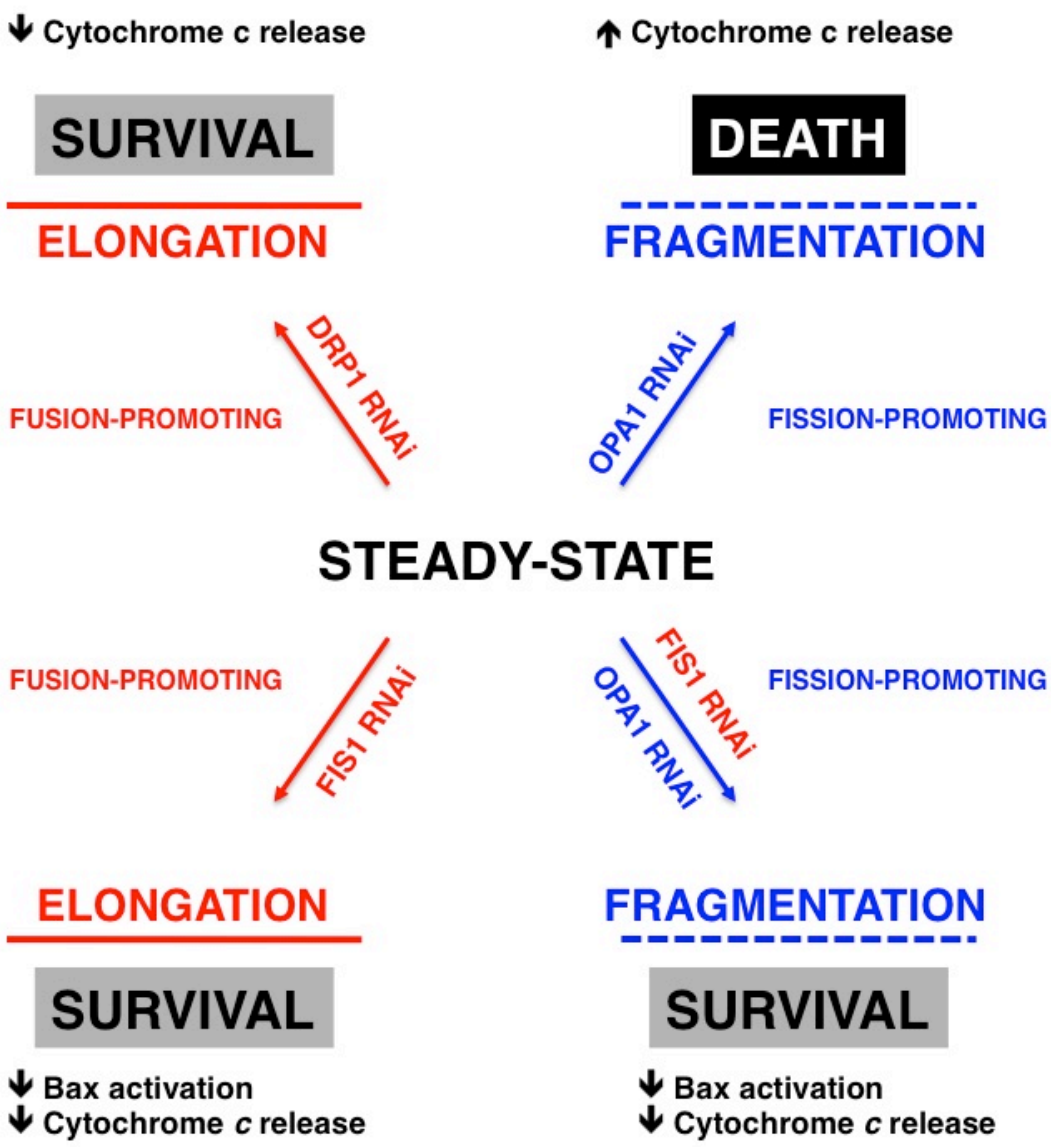
↓ Cytochrome c release
↑ Cytochrome c release
SURVIVAL
DEATH
ELONGATION
FRAGMENTATION
FUSION-PROMOTING
DRP1 RNAi
OPA1 RNAi
FISSION-PROMOTING
STEADY-STATE
FUSION-PROMOTING
FIS1 RNAi
OPA1 RNAi
FIS1 RNAi
FISSION-PROMOTING
ELONGATION
FRAGMENTATION
SURVIVAL
SURVIVAL
↓ Bax activation
↓ Cytochrome c release
↓ Bax activation
↓ Cytochrome c release

Figure 2. Mitochondrial dynamics and the regulation of apoptosis. A general schematic for the effects of the RNAi-mediated genetic knocdown of some of the machinery responsible for mitochondrial dynamics. Downregulation of the fusion protein Opa1 results in the blockage of fusion and leads to a more fragmented network. As a result cells are sensitized to apoptotic-inducers and show increases in cytochrome *c* release and Bax activation as a result. A portion of Opa1 knockdown cells undergo spontaneous apoptosis under steady-state conditions. The additional downregulation of the fission-promoting Fis1 in this setting cannot rescue the fragmented phenotype, however it does rescue cells from the sensitization against apoptotic inducers by decreasing the levels of activated Bax and released cytochrome *c*. On the other side, blocking fission via knockdown of Fis1 alone promotes elongation of the network and provides a strong protection against apoptotic stimuli by blocking both cytochrome *c* release and Bax activation. Similarly, downregulation of the fission-promoting Drp1 gives an elongated phenotype but provides a more moderate protection from death-inducers, reducing only the amount of cytochrome *c* release.

available for oxidative phosphorylation and ATP synthesis [82]. The majority of mitochondrial cytochrome *c* is also sequestered within these IMM structures.

Cristae junctions are structurally maintained by hetero-oligomers of long (IMM-bound) and short (IMS-soluble) isoforms of the pro-fusion protein Opa1 [83]. Mutations in the *opa1* gene cause a human neuropathy resulting in the loss retinal ganglion cells, known as dominant optic atrophy [84]. The soluble form of Opa1 is a result of the proteolytic processing by the integral membrane presenilin-associated rhomboid-like (Parl) protein [85]. During MOMP, extensive changes to these IMM structures are required in order to release cytochrome *c* from mitochondria. It has been shown *in vitro* that tBid causes the disassembly of Opa1 hetero-oligomers, resulting in the widenening of cristae junctions and the mobilization of the bulk of cytochrome *c* out of mitochondrial cristae [86]. Furthermore, the tBid-induced Opa-1 complex disassembly and the opening of cristae junctions is caspase independent and requires Bax recruitment to the OMM [87]. The sensitization to apoptotic inducers observed with down-regulation of Opa1 is therefore likely due to a lack of cristae junctions and is independent of its role in IMM fusion [83, 88]. The necessity of Parl in Opa1-mediated cristae junction maintenance is highlighted by studies in Parl knockout mice that show increased sensitization to intrinsic apoptotic stimuli due to a lack of soluble Opa1 [85]. Therefore Opa1 is a regulator of the intrinsic apoptotic pathway upstream of caspase activation.

1.5 Ubiquitin-mediated regulation of apoptosis

Ubiquitination is a post-translational modification that affects a variety of cellular functions. It is most well known to regulate protein levels by triggering their degradation through the 26S proteosome but it also plays many signaling roles within the cell including lysosomal internalization and targeting, modulation of protein interactions, changes in protein localization, transcriptional regulation, DNA repair and transmembrane signaling [89].

The targeting of a protein for mono- or poly-ubiquitination is a multi-step process. First, the ubiquitin-activating enzyme (E1) forms a thioester bond with the ubiquitin molecule. The activated ubiquitin is then transferred to a cysteine residue on the ubiquitin-conjugating enzyme (E2). Finally, a direct interaction between the ubiquitin ligase (E3) and the E2 permits the transfer of ubiquitin to the target molecule [90]. This occurs through the isopeptide bond formation between the C-terminal glycine residue on the ubiquitin molecule to a lysine residue on the target protein. The two main classes of poly-ubiquitination are determined by the lysine of the ubiquitin moiety used for bond formation. Lysine-48 (K48) linkages cause the target protein to be proteolytically degraded following conjugation of at least four ubiquitin molecules [91]. Lysine-63 (K63) linkages on the other hand are involved in signaling and directing protein localization [92].

The majority of E3 ligases can be divided into two classes. The first being the homologous to the E6-AP carboxyl terminus (HECT) domain-containing that require the formation a thioester intermediate between ubiquitin and the active-site cysteine of the E3 [93]. The second class of E3's contains the really interesting new gene

(RING) finger domain that, unlike HECT ligases, does not form a ubiquitin intermediate. RING finger E3 ubiquitin-ligases are estimated to be encoded by more than 600 mammalian genes [94]. Zinc ion coordination by a specific cysteine and histidine ($Cys_3HisCys_4$) amino acid motif is a characteristic of RING finger proteins that aids in the transfer of the ubiquitin moiety from the E2 [95, 96]. RING ligases have been shown to function as monomers, homo- or hetero-dimers, as well as in multi-subunit complexes [89].

E3 ubiquitin-ligases are currently emerging as key regulators of apoptosis. This is due, in part, to the high degree of specificity conferred by the E3 in the recognition of the target protein [97]. Because of the wide-ranging effects across different cellular processes, ubiquitin-mediated signaling allows for the regulation of the intrinsic pathway at multiple levels. This includes the transcriptional regulation of apoptotic gene expression, the regulation of Bcl-2 family protein levels, the regulation of mitochondrial quality control and therefore ultimately the control of MOMP and caspase activation [98]. The classic example of controlled apoptotic gene expression is the ubiquitination of the tumor suppressor p53 by the RING-containing murine double minute-2 (Mdm2) protein [99]. Mdm2 is classified as an oncogene because of its increased expression in several tumors and its ability to decrease p53 levels, thereby inhibiting transcriptional activation of pro-apoptotic genes and blocking death [100, 101]. Another example of E3's that regulate cell death include the inhibitors of apoptosis proteins (IAPs). The IAPs are RING-finger proteins that act downstream of MOMP by targeting caspases for proteosomal degradation, thereby also inhibiting death [89, 102, 103]. Furthermore, the IBR-type

RING-finger E3 ubiquitin ligase (IBRDC2) has been shown to down-regulate Bax protein levels, possibly serving to protect cells from the spontaneous activation of Bax. IBRDC2 was found to localize to the cytosol under steady-state conditions but became enriched in mitochondria following apoptotic stimuli in a Bax-dependent fashion [104]. These RING-finger proteins represent only a few examples of E3 ligases that participate in the regulation of the apoptotic program. Based on the vast number of RING ligases encoded by the mammalian genome, there is exists the likely possibility of additional, uncharacterized E3's with similar apoptotic functions.

1.6 Trim family of proteins and their roles as E3 ubiquitin ligases

The tripartite motif (Trim) proteins represent an emerging superfamily of genes with a wide of variety cellular functions. Trim proteins are characterized by the conserved tripartite motif made up of a RING finger, one or two B-box motifs and a coiled-coil region (also known as the RBCC family) [105, 106]. As discussed above, the RING domain confers an E3-ubiquitin ligase activity and is usually found at the N-terminus of Trim proteins [107]. The B-box domain also participates in zinc-binding and has been shown to be involved in a variety of cellular processes such as growth control, differentiation and transcriptional regulation [108]. The coiled-coil domain follows the B-box and is located towards the C-terminus of Trim proteins. It is mainly thought be involved in mediating homo-interactions and in facilitating the formation of larger protein complexes [107].

The cellular functions of some Trim proteins have been characterized. A few of the more well characterized functions include the regulation of estrogen signaling

(Trim25), of transforming growth factor β signaling (Trim33) and of levels of the neuroprotective humanin peptide (Trim11) [109-111]. Efforts to systematically characterize the Trim family have been carried out. Through the overexpression of fluorescently-tagged Trim proteins, the bulk of this family was found to homo-multimerize and to localize in various patterns (diffuse, filamentous, or speckled) within the cytosol or nucleus [112]. Studies of this nature provide some insight into this large protein family but are dependent on the assumption that the addition of a fluorescent tag will not affect protein function or localization. Further characterization of the different members of this family must be carried out, as the cellular functions of the vast majority of Trim proteins are still currently unknown.

Trim17 (also known as terf; testis ring finger protein) is a family member that includes three zinc-binding domains, a RING and two B-boxes, as well as a coiled-coil region. It was originally identified in both human and rat testes using PCR and degenerate primers corresponding to a conserved amino acid sequence in the RING finger domain [113]. Trim17 mRNA has been found to be ubiquitously expressed in embryonic mouse tissues [112]. In adult mouse tissues, its expression has been found to be highest in the spleen, testis and thymus, with detectable levels in brain, kidney and liver [114]. Full length Trim17 is a 54 kDa protein with multiple alternatively spliced human transcript variants and two murine transcript variants reported. The two predominant isoforms for both human and mouse Trim17 differ based on the presence of a C-terminal SPRY (spla and the ryanodine receptor) domain whose function is poorly characterized.

The biological role of Trim17 remained largely unknown until recently. It has been shown to possess ubiquitination activity *in vitro* in the presence of the E2 enzyme UbcH6 (ubiquitin carrier H6). This same study showed that Trim17 is capable of rendering itself susceptible to proteosomal degradation through autoubiquitination [114]. More importantly, Trim17 was recently identified to be involved in the control of neuronal apoptosis upstream of mitochondria. DNA microarray and RT-PCR analysis found Trim17 mRNA to be upregulated in cerebellar granule neurons (CGNs) undergoing the early stages of nutrient-deprivation (potassium/K^+ starvation) induced apoptosis [115]. This upregulation of Trim17 was controlled by the phosphatidylinositol 3-kinase (PI3K) and glycogen synthase kinase 3 (GSK3) pathway. Inhibition of PI3K with the chemical inhibitor LY-2940002 on its own induces neuronal apoptosis [116]. Conversely, inhibition of GSK3 during apoptotic stress protects neurons from death [117]. Consistent with the activation of apoptosis, treatment of CGNs with this PI3K inhibitor produced a concomitant increase in Trim17 mRNA that was blocked with GSK3 inhibition. Additionally, overexpression of Trim17 alone was found to initiate apoptosis in CGNs in a Bax-dependent manner [118]. These data suggest a role for Trim17 as a regulator of apoptosis, particularly in a neuronal setting.

Currently, only a few potential interacting partners of Trim17 have been identified. Another E3-ligase and Trim family member, Trim44, was found in a yeast two-hybrid screen and was shown to interact with Trim17 via the coiled-coil domains of both proteins [114]. A second yeast two-hybrid screen by the same group identified ZW10 interacting protein (ZWINT), a known component of the kinetochore

complex formed during mitosis, as being a potential substrate for the E3-ligase activity of Trim17. As a result of Trim17 overexpression, ZWINT was found to be downregulated and the growth rate of MCF7 cells was decreased [119].

1.7 Neuronal apoptosis in neurodegeneration

Maintenance of mitochondrial function and integrity is critical to neuronal survival. The high-energy (ATP) demands in neurons are a result of the numerous protein kinase reactions that mediate synaptic signaling, excitability and the associated long-term alterations in neuronal structure and function required for cell survival [120]. In addition to being the major energy source within neurons, mitochondria play several other crucial roles in neurons. The dynamic nature of mitochondria allow for their movement across neuronal axons and dendrites. As in other cell types, mitochondria aid in the regulation of calcium and redox signaling as well as the initiation of apoptosis in neurons.

Mitochondrial dysfunction and the upregulation of apoptosis is a hallmark of numerous neurodegenerative diseases including Alzheimer's, Parkinson's, and Huntington's diseases as well as stroke, amyotrophic lateral sclerosis and some psychiatric disorders [121]. In the context of stroke, or cerebral ischemia, a restriction in blood flow to an area of the brain results in impaired glucose and oxygen delivery to neurons in the affected region. In a neuron, this rapidly leads to ATP-depletion and sets off a cascade of signaling events characterized by increased intracellular calcium and ROS. The binding of glutamate to ionotropic NMDA (N-methyl-D-aspartate) and AMPA (α-amino-3-hydroxy-5-methyl-4-isoxazolepropionic

acid) receptors facilitates further increases in calcium flux into the cell [122]. These changes ultimately trigger MOMP, caspase activation and eventually cell death through the intrinsic pathway as in other cell types.

The pro-apoptotic Bcl-2 protein Bid plays a central role in neuronal apoptosis. As described in previous sections, Bid assumes its pro-apoptotic function after proteolytic cleavage by caspase 8 to generate tBid. The caspase-independent cleavage of Bid has been shown to occur in some neuronal cell death situations and is mediated by calpains, granzyme B or lysosomal hydrolases [123, 124]. Regardless of the way in which Bid becomes activated, the generation and translocation of tBid to the OMM have been shown in many examples of neurodegeneration, including stroke [125]. In vivo, tBid has been detected as early as 4-hours following middle cerebral artery occlusion, an experimental model of stroke [126]. Loss of Bid *in vivo* has shown to be protective against a variety of neuronal insults. Bid knockout mice show a reduction in caspase 3 activation and a resistance from secondary brain injury following physical trauma in addition to a reduction in infarct size *in vivo* following focal ischemia [126, 127]. Futhermore, Bid-deficient neurons are highly resistant against oxygen-glucose deprivation (OGD) induced cytochrome *c* release [128]. Bax activation and MOMP have therefore been suggested to be important steps in neuronal apoptosis because of their connection to tBid.

Three main targets within the intrinsic death pathway have been proposed for stroke therapy: caspases, AIF, and Bid. Peptide inhibitors of caspases have showed some protection against OGD, however current inhibitors have limited

therapeutic potential due to their inability to cross the blood-brain-barrier [129]. Down-regulation of AIF has proved protective against acute ischemia and trauma, but long-term inhibition has been suggested to impair the function of respiratory chain complex I, thereby reducing cell viability [130]. Additionally, the upstream mitochondrial dysfunction that occurs during apoptosis, even in the presence of AIF or caspase inhibition, can give rise to a necrotic-like death in neurons, primarily due to ATP depletion [131, 132]. The most promising therapeutic target to date appears to be Bid. Small molecule compounds that bind to the surface of Bid have been shown to preserve mitochondrial function, prevent Smac release, and block caspase 3 activation [133]. The centrality of Bid and tBid in the intrinsic death pathway makes the identification of additional events upstream of Bax a particularly attractive avenue for the development of new therapeutic approaches.

Currently, there is emerging evidence for other regulators of neuronal cell death upstream of MOMP. Recently, a role for Opa1 in regulating neuronal survival in a Parkinson's disease-related model has been proposed. The use of parkinsonian neurotoxins led to an oxidative-dependent disruption of Opa1 complexes at cristae junctions and the movement of cytochrome *c* from within cristae to the IMS. As a result these cells were primed for death through the intrinsic pathway [134]. These data provide rationale for the upregulation of Opa1 levels as a means to confer protection against apoptotic insults in neurons. Moreover, Trim17 has been shown to promote apoptosis in CGNs but its role in cortical neurons has yet to be investigated. Ischemic injury to the cerebral cortex is the most common form of stroke whereas cerebellar infarction represents less than 4% of all cases

[135, 136]. Therefore, in the context of stroke, the function of Trim17 in cortical neuron death warrants further investigation.

1.8 Hypothesis and objectives

Based on preliminary data obtained in two genetic pilot screens looking for novel regulators of Bax activation, I hypothesize that Trim17 regulates Bax-dependent apoptosis. The objectives of my thesis are to establish that Trim17 regulates cell death in cortical neurons in response to tBid overexpression and to determine the molecular mechanism by which this is achieved. In order to address the latter, I aim to use unbiased proteomic approaches to identify protein interactor(s) and/or substrate(s) of Trim17.

Chapter 2: Materials & Methods

2.1 Genetic screens to identify novel regulators of Bax activation

Two independent screens were carried out to identify novel genes involved in Bax activation. Each screen looked at approximately 900 genes in the human genome. Details of each screen are described below.

2.1.1 Screen 1: Hela cells overexpressing YFP-Bax

Hela cells with a tetracycline-inducible YFP-Bax were maintained in Dulbecco's Modified Eagle Medium (DMEM) supplemented with 10% tetracycline-free fetal calf serum (FCS, Clontech) and 100 units/ml penicillin (Hyclone), and 100 ug/ml streptomycin (Hyclone). Cells were reverse transfected (Lipofectamine RNAiMAX, Invitrogen) in 384-well plates (Falcon) with pools of four siRNA duplexes (10 nM total) per gene. After 72 hours, cells were infected with Adenovirus expressing HA-tBid (Ad-tBid) and were co-treated with 10 uM of the pan-caspase inhibitor Q-VD-OPh (QVD, Calbiochem) for 8 hours. Cells were fixed and immunostained against the outer mitochondrial membrane protein Tomm20. Cells were imaged with the ArrayScan VTI HCS (Thermo Scientific) inverted microscope using a 40X objective. Images were analyzed using the Cellomics software (Thermo Scientific). An algorithm was developed to measure the amount of YFP-Bax fluorescence that did not colocalize with Tomm20 staining and was therefore deemed to be "inactive". This was termed the percentage of cytoplasmic YFP-Bax.

2.1.2 Screen 2: U2OS cells immunostained against active Bax

Osteosarcoma (U2OS) cells were maintained in McCoy's 5A Modified Media (Thermo) supplemented with 10% FCS (Hyclone), 100 units/ml penicillin and 100 ug/ml streptomycin. Cells were reverse transfected and infected with Ad-tBid as described above (2.1.1). Cells were fixed and immunostained against Tomm20 and active Bax (6A7). Imaging and analysis were performed as described above (2.1.1). An algorithm was developed to measure the amount of 6A7 fluorescence that colocalized with mitochondria (Tomm20 staining). This was termed the intensity of active Bax.

2.2 Generation of shRNA-expressing lentivirus

shRNA targeting the coding sequence of murine Trim17 or a non-targeting control were inserted into the pLKO.1 vector at the AgeI and EcoRI sites within the multiple cloning site. Lentiviral particles were generated in HEK293T cells. Cells were transfected using polyethylenimine with the pLKO.1 vector of interest along with the viral packaging plasmids pMD2.G and pCMV6.4. The viral supernatant (SN) was collected 72 hours following transfection. The SN was then centrifuged at 300g for 5 minutes at 4^{o}C, then passed through a 0.2 μm filter. The viral SN was further concentrated by ultracentrifugation with a 20% sucrose cushion. The SN following the high-speed spin was discarded and the viral pellet was resuspended in a small volume of neurobasal media (Gibco).

2.3 Cell culture of mouse embryonic cortical neurons

Pregnant CD1 mice (E13) were sacrificed by cervical dislocation. Cortical neurons were isolated from embryos as described previously [137]. Cells were seeded in neurobasal media supplemented with 125 mM L-glutamine (Hyclone), 5 units/ml penicillin, 5 ug/ml streptomycin, B27 (Invitrogen) and N2 (Invitrogen) in poly-D-lysine (50 ug/ml, Sigma) coated plates. Lentivirus infection was done at the time of seeding with a 50% media exchange 5 hours later. Cells were maintained at 37ºC in 5% CO_2 and were half fed with fresh neurobasal media every 3 days. The mitotic inhibitor cytosine β-D-arabinofuranoside (Sigma) was added, at a concentration of 5 uM in 384-well plates or 10 uM in all other plate formats, 24 hours after seeding to inhibit glial cell proliferation. All functional experiments were done after 5 days *in vitro* (DIV = 5).

2.4 Assay for cell death in cortical neurons

Cortical neurons in 384-well plates (Greiner) were treated with Ad-tBid in complete neurobasal media containing 0.05 ug/ml Hoechst. Some samples were co-treated with 30 uM QVD (Calbiochem) to ensure that Ad-tBid was eliciting an apoptotic response. Cells were incubated for 30 minutes at 37ºC prior to beginning automated confocal imaging (Opera, Perkin-Elmer) of 25 fields per well with a 20X objective. Cells were imaged for up to 30 hours (in 5% CO_2 at 37ºC) following Ad-tBid infection. Images were analyzed using a computer-generated algorithm to measure nuclear size and morphology (Columbus, Perkin-Elmer). Nuclei with a round morphology of a minimum size were termed “healthy nuclei”. The number of

healthy nuclei in a given sample was normalized to the number in that same sample at time 0 and was reported as the percentage of basal healthy nuclei.

2.5 TMRE and ATP measurements in cortical neurons

Cortical neurons in 384-well plates were treated with QVD-alone or Ad-tBid and QVD as described above (2.4) for 8, 16 and 20 hours. Prior to imaging, cells were incubated with 100 nM of MitoTracker® Green FM (Invitrogen) and 0.05 ug/ml Hoechst in neurobasal media for 45 minutes. Cells were then incubated for 15 minutes with 10 nM of tetramethylrhodamine ethyl ester dye (TMRE, Invitrogen). Confocal images of 10 fields per well were taken at a single time point using a 20X objective. Images were analyzed with a computer-generated algorithm that uses the MitoTracker® Green staining area around the nucleus to define a mitochondrial region. The intensity of TMRE fluorescence within this region was determined. The number of cells with TMRE intensity above a threshold value were termed “TMRE-positive nuclei”. For measurements of ATP levels, neurons were treated as described above for 20 hours, after which the CellTiter-Glo reagent was added directly to cells (Promega) and luminescence was then measured (Synergy plate reader, Biotek).

2.6 OCR measurements in cortical neurons

The Seahorse XF-24 Extracellular Flux Analyzer (Seahorse Bioscience) was used to measure the oxygen consumption rate (OCR) in cortical neurons. Cortical neurons were seeded in Seahorse XF-24 cell culture plates and were treated with

QVD-alone or with Ad-tBid and QVD in combination (as described above) for 10 or 20 hours. Following tBid treatment, a mitochondrial stress test was performed. Cells were serially treated with four different mitochondrial poisons (all at 2 uM, Seahorse Bioscience): (1) oligomycin, (2) trifluorocarbonylcyanide phenylhydrazone (FCCP), (3) antimycin A and (4) rotenone. Following the assay, cell lysates were collected in SDS sample buffer (62 mM Tris base, 10% glycerol, 2% SDS) and protein was quantified by BCA assay (Pierce). OCR measurements were normalized to the total amount of protein in each sample.

2.7 Proteomic screen I: HEK293 Flp-In TRex cells

cDNA encoding wild-type (WT) Trim17 was cloned into the Gateway-compatible 3x-FLAG-pDEST-FRT/TO vector. Quickchange PCR using the WT template and mutagenic primers was done to generate the C16A point mutant. Stable cells were produced by forward transfection (Jetprime, Polypus) of either vector control, WT or C16A Trim17 alongside the Flp-recombinase vector (pOG44) in the tetracycline-inducible HEK293 Flp-In TRex cell line. Stably transfected cells were selected for with 5 ug/ml blasticidine and 200 ug/ml hygromycin (Sigma). Cells were maintained in DMEM supplemented with 10% tet-free FCS (Clontech), 100 units/ml penicillin and 100 ug/ml streptomycin. For optimization experiments, FLAG-immunoprecipitation (IP) was done using mouse anti-FLAG-M2 conjugated agarose beads (Sigma) or Protein A/G beads (Santa Cruz). Expression of 3xFLAG-Trim17 was induced with 1 ug/ml tetracycline (tet) for 40 hours. Cells were treated with either vehicle control (DMSO) or 5 uM etoposide for 2 hours prior to harvesting for

FLAG-immunoprecipitation (IP) and multidimensional protein identification technology (MudPIT) mass spectrometry (MS) analysis (Dr. A.C. Gingras).

2.8 Proteomic screen II: GST-RING-TRIM17 and mouse brain lysates

cDNA encoding the RING domain of WT Trim17 was cloned into the pGEX-5x-2 glutathione S-transferase (GST) expression vector. Recombinant GST-RING-Trim17 and the GST-only control were expressed in *E. coli* (BL21 strain) and purified over glutathione sepharose 4B (GE Life Sciences). Mouse brain lysates were prepared from wild type FVB mice as described previously [138]. CHAPS (instead of Tx100) was added after tissue homogenization to further solubilize proteins. Soluble S2 fractions (10 mg protein per sample) were incubated with ~40 ug of either GST-control or GST-RING on glutathione sepharose beads for 5 hours at 4ºC. Beads were then washed with a Tris-buffered salt solution and protein was eluted by boiling samples in SDS sample buffer (62 mM Tris base, 10% glycerol, 2% SDS, ~18 mM bromophenol blue, 1mM DTT) at 95ºC for 5 minutes. GST-protein alone and GST-protein incubated with lysate samples were resolved by SDS-PAGE and proteins were visualized by silver-stain (Pierce). Protein bands that appeared unique to the GST-RING with lysate sample were cut, gel extracted and subjected to MS analysis (Dr. A.C. Gingras). Hits were validated by WB with antibodies against NSF, Opa1 and tubulin.

2.9 FLAG-immunoprecipitation from HEK293 Flp-In TRex cells

HEK293 Flp-In TRex cells were collected in non-ionic detergent co-IP buffer (25 mM Tris pH 7.5, 150 mM NaCl, 50 mM NaF, 0.5 mM EDTA pH 8.0, 0.5% CHAPS, 5 mM β-glycerophosphate, 5% glycerol, 1mM DTT, Pierce Halt protease inhibitor cocktail). Cells were freeze-thawed to aid in lysis prior to centrifugation at 10,000g for 20 minutes at 4ºC. The soluble fractions were incubated with anti-FLAG-M2 conjugated agarose beads overnight at 4ºC. Beads were then centrifuged at 10,000g for 1 minute at 4ºC. The SN was discarded and beads were washed with co-IP buffer containing 150 mM NaCl (1 wash), 500 mM NaCl (3 washes) followed by a final rinse with dH_2O. Beads were dried completely and protein was eluted by boiling at 95ºC for 5 minutes in SDS sample buffer.

2.10 Subcellular fractionation of cortical neurons

Cortical neurons were isolated and cultured as described above (2.3). Neurons were trypsinized (0.25%, Life Technologies) and harvested in FCS-containing DMEM. Cells were centrifuged at 300g for 5 minutes at 4ºC. The cell pellet was rinsed with ice-cold PBS and centrifuged again as above. The SN was discarded and cells were resuspended in mitochondria resuspension buffer (MRB; 200 mM mannitol., 68 mM sucrose, 20 mM Hepes pH 7.4, 80 mM KCl, 0.5 mM EGTA, 2 mM $Mg(Acetate)_2$, Pierce Halt protease inhibitor cocktail). Cells were broken using a cell cracker with 8.006 mm ball. The broken cell suspension was centrifuged at 3,000 rpm for 10 minutes at 4ºC to pellet nuclei and unbroken cells. The post-nuclear SN was centrifuged a second time to remove any nuclear

contaminants prior to centrifugation at 10,000 rpm for 10 minutes at 4ºC. The post-mitochondrial SN was removed and the mitochondrial pellet was washed 3 times with MRB. The protein concentration of samples was determined by BCA assay prior to SDS-PAGE.

2.11 SDS-PAGE & Western blot analysis

Protein lysates were harvested in SDS sample buffer. SDS-PAGE was performed in Tris-glycine buffer. For Western blotting, proteins were transferred to 0.4 μm polyvinylidene fluoride (PVDF) membranes (Millipore) in Tris-glycine buffer supplemented with methanol. Following transfer, membranes were blocked with 5% milk in Tris-buffered saline (TBS) supplemented with 1% Tween (Sigma) (TBS-T) for either 1 hour at room temperature or overnight at 4ºC. Primary antibodies were incubated for either 1 hour at room temperature or overnight at 4ºC (Table 1). Following incubation with primary antibodies, membranes were washed with TBS-T for 30 minutes to 1 hour. Secondary antibodies were incubated at a concentration of 1:5,000 for 1 hour at room temperature. Following this membranes were washed again, as above with TBS-T, prior to detection with enhanced chemiluminescence (ECL or ECL-Prime, GE Life Sciences).

Table 1. List of primary antibodies

Primary antibody	Species	Dilution	Company/collaborator
Active Bax (6A7)	Mouse	1:1,000 (for IF)	Dr. D. Andrews
β-actin	Mouse	1:10,000	Biorad
β-subunit	Mouse	1:2,000	Abcam
Calnexin	Rabbit	1:1,000	Abcam
GAPDH	Mouse	1:1,000	GeneTex
GST:GFP	Rabbit	1:1,000	

FLAG	Mouse	1:1,000	Sigma
FLAG-HRP	Mouse	1:1,000	Sigma
OPA1	Mouse	1:1,000	BD Bioscience
OPA1	Rabbit	1:1,000	Abcam
NSF	Rabbit	1:1,000	Cell Signaling
TOMM20	Rabbit	1:2,000 (for IF)	Santa Cruz
TRIM17	Rabbit	1:250	Santa Cruz
Tubulin (α)	Rabbit	1:1,000 (for IF & WB)	Santa Cruz
Tubulin (β)	Mouse	1:5,000	Dr. S. Beug
V5	Mouse	1:500 (for IF & WB)	Invitrogen

2.13 Immunofluorescence

Cells were fixed in 3.7% formaldehyde containing 5 ug/ml Hoechst (Invitrogen). Cells were washed with 3% glycine in PBS, permeabilized with 0.1% Triton X-100 (Tx100, Sigma) and blocked with 3% bovine serum albumin (BSA, Sigma) in PBS for 1 hour at room temperature or overnight at 4ºC. Primary antibodies (Table 1) were added in 3% BSA in PBS and incubated for 1 hour at room temperature or overnight at 4ºC. Secondary antibodies (AlexaFluor, Invitrogen) were added at either 1:2000 or 1:4000 in 3% BSA in PBS and incubated for 1 hour at room temperature.

2.14 Statistical analysis

All data are expressed as mean +/- standard error of means (SEM). Unless otherwise stated, all results were obtained through a minimum of three independent experimental replicates, with the exception of the pilot screening data (single experiment, samples in triplicate). The student's t-test (two-tailed, type 2) was used to determine data significance.

Chapter 3: Results

3.1 Pilot screens for regulators of Bax activation

With a view to perform a full genome screen to identify novel genes that regulate Bax activation, two independent pilot screens each looking at approximately 900 genes in the human genome were first carried out. The first screen, done in Hela cells, showed a ~30% reduction in the amount of cytoplasmic, or inactive, YFP-Bax when control cells were treated with tBid. Trim17 knockdown cells showed a significantly higher amount of cytoplasmic YFP-Bax in the presence of tBid compared to controls (Figure 3B). The second screen, done in U2OS cells, showed a ~11-fold increase in the fluorescent intensity of the conformation-specific 6A7 antibody that recognizes active Bax in tBid-treated control cells (Figure 3C). Once again, cells with reduced Trim17 showed a ~40% reduction in Bax activation. The results of these two independent pilot screens show that tBid-induced Bax activation is impaired in the absence of Trim17. Taken together, these results suggest that Trim17 regulates the intrinsic pathway of apoptosis upstream of Bax activation.

3.2 Loss of Trim17 delays cell death in cortical neurons

Previous studies have shown that Trim17 mRNA is upregulated in potassium-starved CGNs undergoing apoptosis [118]. Based on these data and the preliminary screening results obtained in our lab, I sought to further investigate the role of Trim17 in neuronal cell death. With the aim of examining Trim17 biology in a model more relatable to cerebral ischemia than CGNs, I chose to determine the effect of down-regulation of Trim17 on sensitivity of an apoptotic stimulus in cortical neurons.

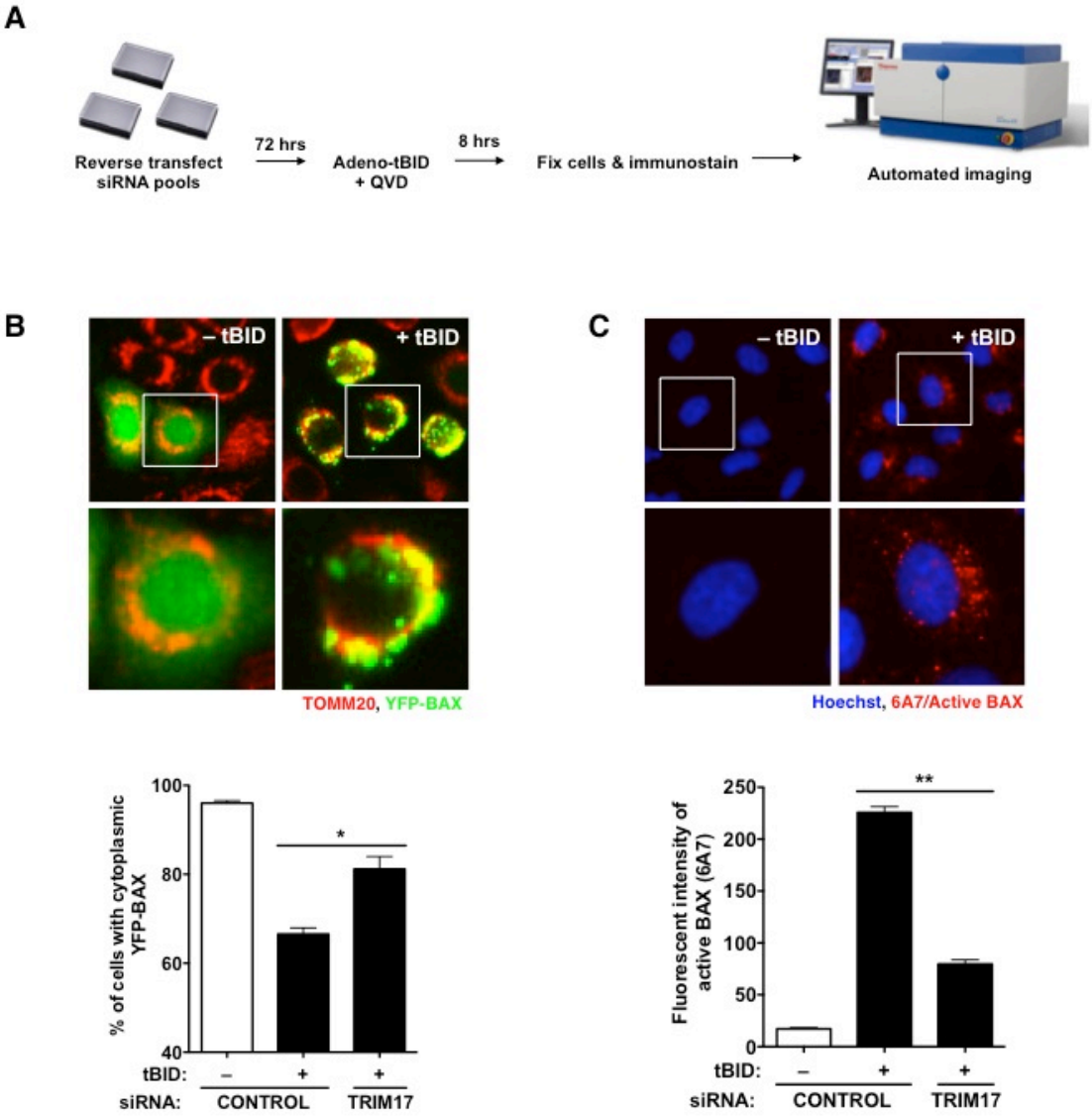
A
Reverse transfect siRNA pools
72 hrs
Adeno-tBID + QVD
8 hrs
Fix cells & immunostain
Automated imaging
B
– tBID
+ tBID
TOMM20, YFP-BAX
% of cells with cytoplasmic YFP-BAX
100
80
60
40
*
tBID: – + +
siRNA: CONTROL TRIM17
C
– tBID
+ tBID
Hoechst, 6A7/Active BAX
Fluorescent intensity of active BAX (6A7)
250
200
150
100
50
0
**
tBID: – + +
siRNA: CONTROL TRIM17

Figure 3. Two independent pilot genetic screens identify TRIM17 as being required for Bax activation. A. High-throughput screen workflow. B. Fluorescent images showing siControl Hela cells overexpressing YFP-Bax treated with control or Adenovirus overexpressing tBID and stained against the outer mitochondrial membrane marker protein TOMM20. Quantification of the percentage of cells that retain cytoplasmic YFP-BAX is shown below (Screen 1, $*p < 0.01$). C. Fluorescent images showing siControl U2OS cells infected with Adeno-tBID and stained against the active form of BAX (6A7) and TOMM20. Quantification of the fluorescent intensity of 6A7 is shown below (Screen 2, $**p < 0.001$).

In order to address this question, lentivirus expressing shRNA against murine Trim17 was generated. Cortical neurons were infected with shControl or shTrim17 lentivirus and subjected to Western blot analysis. The shRNA against Trim17 targets a C-terminal region of murine Trim17 absent in the short isoform but was found to give a 60-70% reduction in the long isoform (~54 kDa) of Trim17 (Figure 3A).

In order to monitor the kinetics of cell death in neurons, an assay was developed using an automated confocal microscope. Live cells were incubated with a low concentration of Hoechst stain to visualize nuclei. Hoechst concentrations below 0.2 ug/ml were found to be non-toxic to cells, however concentrations as low as 0.05 ug/ml were found to be sufficient for imaging (Appendix A). This approach facilitated the extensive imaging of several samples over a long period of time and also to reduced the background signal from the Hoechst and phenol red in the growth medium.

In control cells, tBid caused a significant decrease in the number of nuclei with normal, or “healthy”, morphology and a subsequent increase in the number of condensed, or apoptotic nuclei beyond ~16 hours of overexpression (Figure 4B,C). To confirm that the Adeno-tBid was in fact triggering an apoptotic response, some cells were co-treated with the pan-caspase inhibitor QVD. Co-treatment with tBid and QVD was found to delay neuronal death up to ~24 hours (Figure 4C). Beyond this point cells underwent a caspase-independent form of cell death.

Next, the effect of Trim17 downregulation on tBid-induced neuronal death was examined. Knockdown of Trim17 delayed cell death by ~4 hours compared to

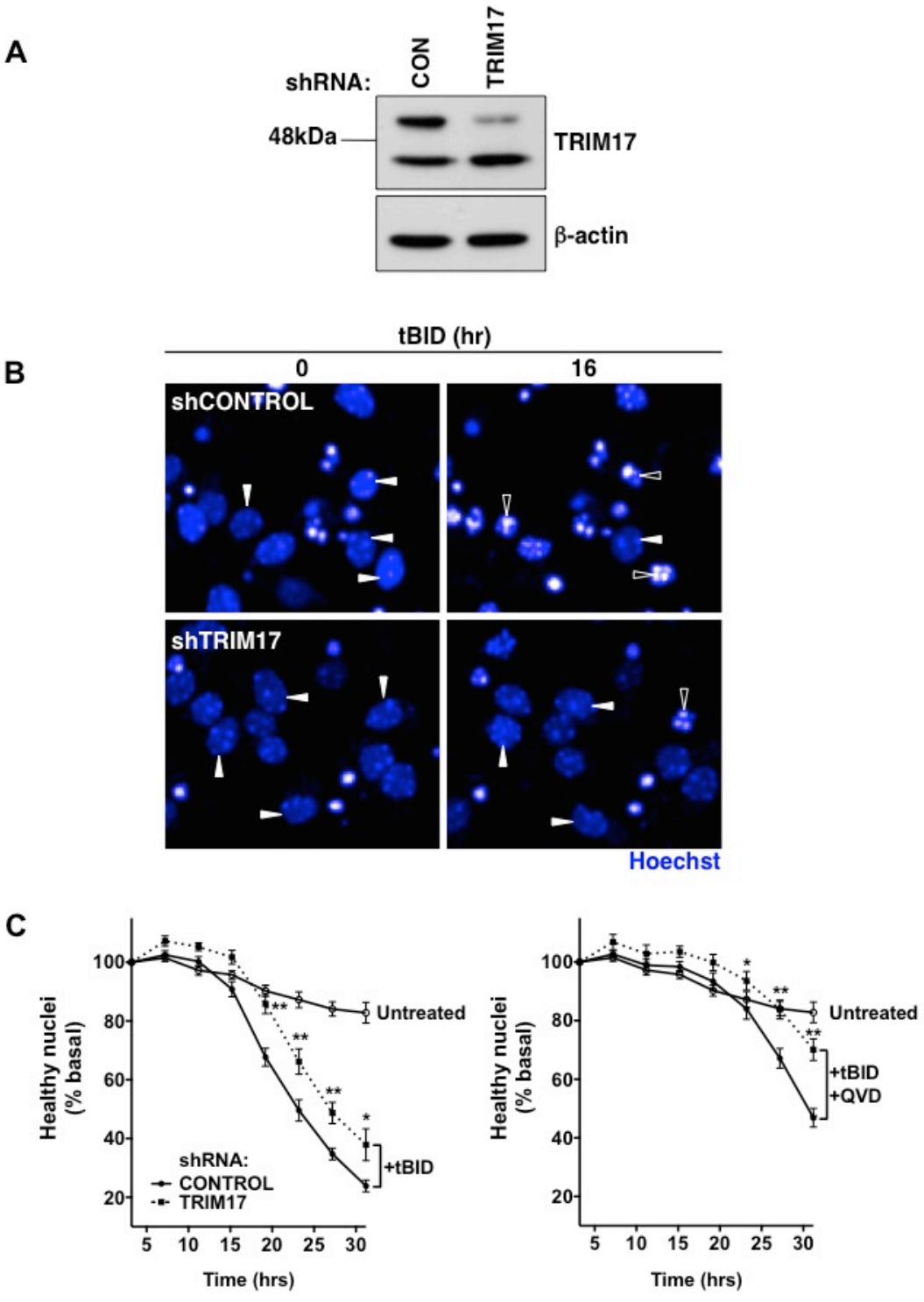
A
shRNA:
CON
TRIM17
48kDa
TRIM17
β-actin
B
tBID (hr)
0
16
shCONTROL
shTRIM17
Hoechst
C
Healthy nuclei (% basal)
Time (hrs)
Untreated
+tBID
shRNA:
CONTROL
TRIM17
+tBID
+QVD

Figure 4. Knockdown of TRIM17 delays cell death in cortical neurons. A. Western blot showing shRNA-mediated knockdown of TRIM17. B. Fluorescent confocal images showing Hoechst-stained live shControl or shTRIM17 neuronal cultures at 0 & 16 hr post-Adeno-tBID infection. Healthy nuclei are indicated by solid white arrowheads, condensed nuclei are indicated by hollow white arrowheads. C. Quantitative analysis of time course for neuronal survival in response to tBID overexpression as measured by Hoechst-staining for nuclear morphology. Knockdown of TRIM17 gives a significant delay in cell death as compared to control cells treated with tBID (*$p < 0.01$, **$p < 0.001$).

control cells (Figure 4B,C). The delay in cell death observed in Trim17 knockdown cells was similar to that observed in control cells co-treated with QVD. The combination of Trim17 knockdown and QVD-treatment gave an additive protection against cell death (Figure 4C). These results show that neuronal death is delayed but not blocked as a result of reduced Trim17 expression. These data are consistent with a requirement of Trim17 in tBid-induced Bax activation.

3.3 Mitochondrial function is maintained after tBid in Trim17 knockdown neuronal cultures

As shown above, Trim17 knockdown neurons are resistant to tBid-induced cell death. This led me to question whether knockdown cells are also resistant to mitochondrial outer membrane permeabilization (MOMP) and the general mitochondrial dysfunction that are normally observed with the onset of the intrinsic apoptotic program [16]. To determine this, the effect of tBid overexpression on mitochondrial function was assessed in cortical neurons by three independent methods.

First, mitochondrial potential ($\Delta\Psi$) was measured using the potentiometric fluorescent dye tetramethylrhodamine ethyl ester (TMRE). TMRE fluorescence, or $\Delta\Psi$, was found to decrease in control cells beyond 16 hours of tBid-treatment (Figure 5A,B). This loss of $\Delta\Psi$ was not as severe in Trim17 knockdown cells, even at the later time point of 20 hours of tBid-treatment (Figure 5B). This suggests that downregulation of Trim17 allows for the maintenance of $\Delta\Psi$-generating electron

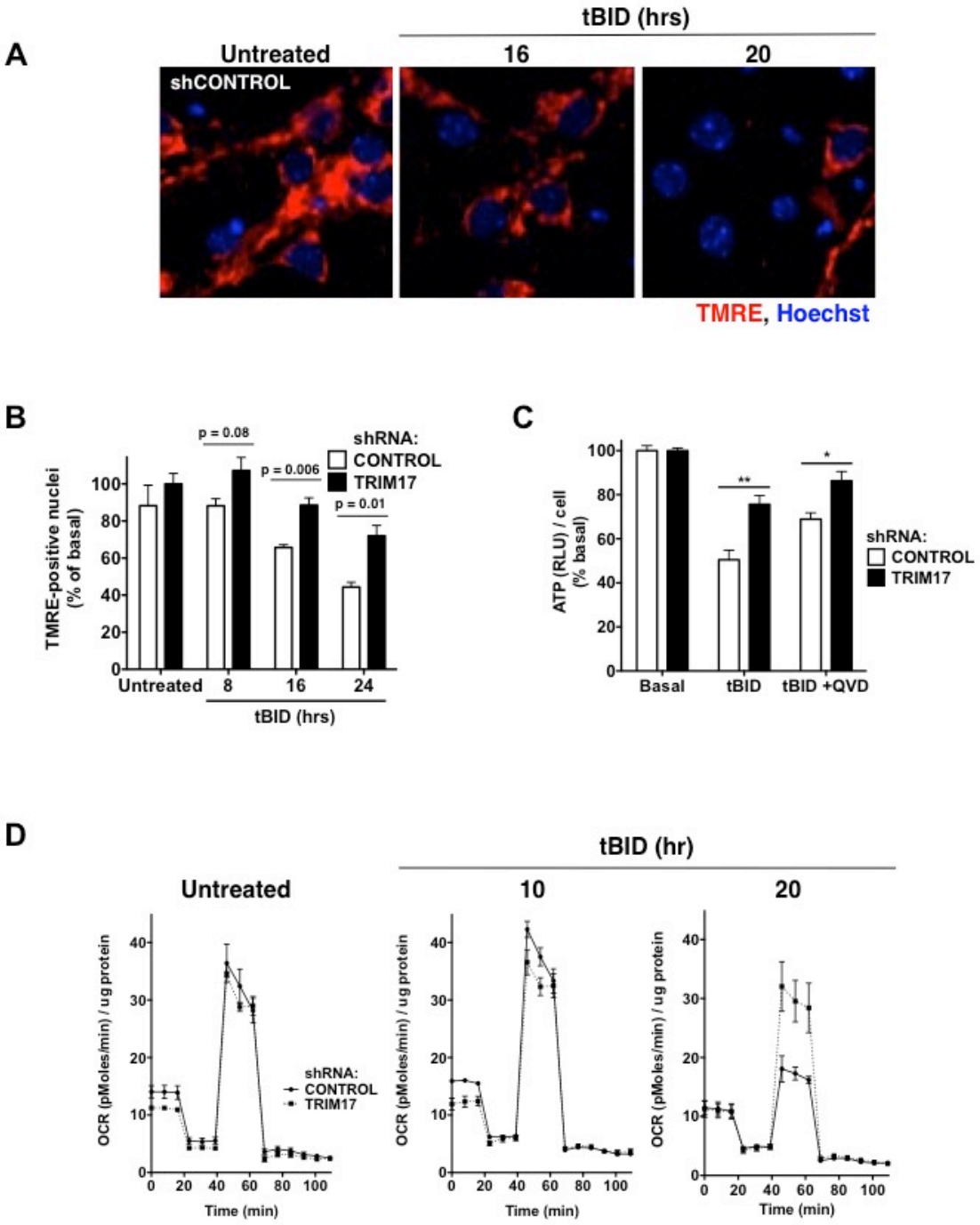
A
tBID (hrs)
Untreated
16
20
shCONTROL
TMRE, Hoechst
B
TMRE-positive nuclei (% of basal)
p = 0.08
p = 0.006
p = 0.01
shRNA:
CONTROL
TRIM17
Untreated
8
16
24
tBID (hrs)
C
ATP (RLU) / cell (% basal)
**
*
shRNA:
CONTROL
TRIM17
Basal
tBID
tBID +QVD
D
tBID (hr)
Untreated
10
20
OCR (pMoles/min) / ug protein
shRNA:
CONTROL
TRIM17
Time (min)

Figure 5. Mitochondrial function is maintained in the presence of tBID in TRIM17 knockdown neuronal cultures. A. Fluorescent confocal images showing TMRE loading in non-treated or tBID-treated shControl cells. B. Histogram showing quantification of the percentage of cells with that maintain membrane potential ($\Delta\Psi$) as measured by TMRE fluorescence intensity (>120). Loss of $\Delta\Psi$ in response to tBID is delayed in TRIM17 knockdown cultures. C. Histogram showing ATP levels are protected to levels comparable to the QVD-treated sample in TRIM17 knockdown cells in response to tBID overexpression. D. Oxygen consumption rate (OCR) measurements under control conditions and after 12 or 20 hr of tBID-overexpression. Maximal respiration is maintained in knockdown cells after 20 hr of tBID-overexpression compared to control cells. These tracings are from a single experiment and are representative of three independent experimental replicates. (*$p < 0.01$, **$p < 0.001$).

transport within the electron transport chain (ETC).

Second, ATP levels were measured in control and Trim17 knockdown cells under basal conditions or after 20 hours of tBid-treatment in the presence or absence of QVD. Control cells showed a 50% reduction in ATP levels after tBid (Figure 5C). The addition of QVD conferred some protection and resulted in a blunted 30% loss of ATP in control cells. Trim17 knockdown cells were protected from tBID-induced ATP depletion. Furthermore, knockdown cultures obtained a significant additional protection when co-treated with QVD. These results show that, consistent with the maintenance of $\Delta\Psi$, a reduction in Trim17 protein levels allows for functional electron transport and oxidative phosphorylation to continue in the presence of the mitochondrial-stress tBid.

Finally, the oxygen consumption rate (OCR) was measured in control and Trim17 knockdown cells under basal conditions and at two time points (early & late) following tBid treatment (Figure 5D). There was no significant change in OCR levels basally or at the early time point (10 hours post-tBid) in control versus knockdown cells. However, after prolonged tBid exposure, knockdown cultures maintained a higher maximal respiratory capacity (FCCP response) compared to control cells. These OCR data are consistent with the findings described above and support the idea that downregulation of Trim17 prevents the mitochondrial dysfunction normally caused by tBid. These data also further support the role of Trim17 as being upstream of Bax activation and MOMP in the intrinsic death pathway.

3.4 Identification of Trim17 protein-complex members

There is emerging evidence for the importance of E3 ubiquitin ligases as regulators of apoptosis [98]. Currently, only one potential substrate of the E3 ubiquitin ligase activity of Trim17 is known (ZWINT) [119]. I therefore sought to identify a potential interacting partner or substrate that could provide insight as to the mechanism of action of Trim17 in cell death. Two different approaches were used to address this question.

3.4.1 Proteomic approach I: HEK293 Flp-In TRex cells stably expressing 3xFLAG-Trim17

The first approach employed stable cell lines expressing a vector-only control alongside the WT or the catalytically inactive C16A point mutant of 3xFLAG-Trim17. The cells were subjected to FLAG immunoprecipitation (IP) and MS analysis to identify protein complexes specific to the WT (Figure 6A). Prior to this, the screening conditions were optimized for induction of the exogenous protein. The time following tetracycline induction of 3xFLAG-Trim17 expression was determined for both the WT and the C16A mutant by Western blot (WB) analysis. No significant difference between 24 versus 40 hours was observed for the WT but a very slight increase at 40 hours was found for the C16A mutant (Figure 6B). Therefore a 40-hour induction time with tetracycline was chosen for the screen. The optimal concentration of tetracycline was determined to be 1 ug/ml, with higher concentrations providing no increase in the expression of 3xFLAG-Trim17 (Figure 6C). Following this, the specificity of the IP of overexpressed Trim17 to FLAG-

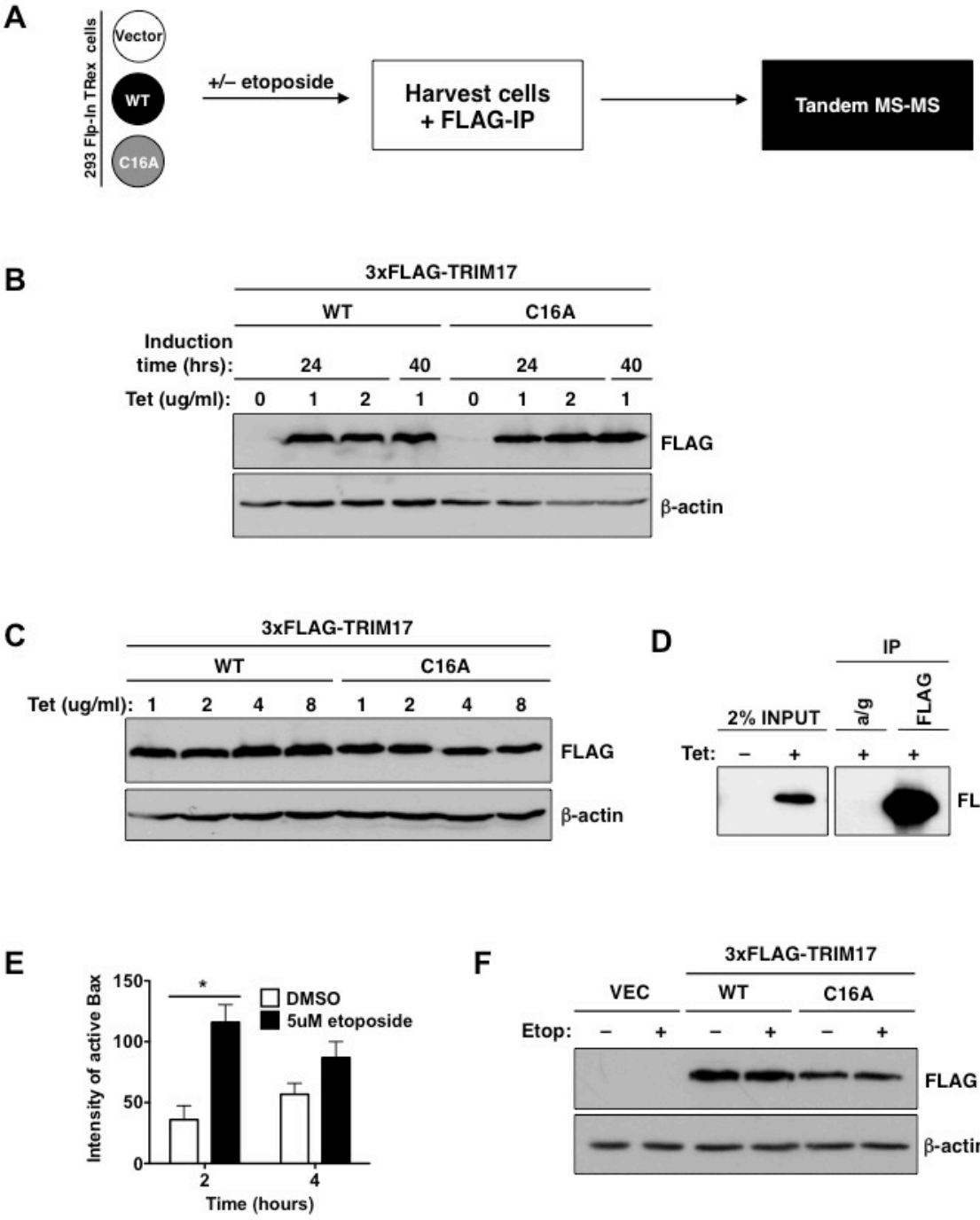
A
293 Flp-In TRex cells
Vector
WT
C16A
+/– etoposide
Harvest cells
+ FLAG-IP
Tandem MS-MS
B
3xFLAG-TRIM17
WT
C16A
Induction time (hrs):
24
40
24
40
Tet (ug/ml):
0 1 2 1 0 1 2 1
FLAG
β-actin
C
3xFLAG-TRIM17
WT
C16A
Tet (ug/ml): 1 2 4 8 1 2 4 8
FLAG
β-actin
D
IP
2% INPUT
a/g
FLAG
Tet: – + + +
FLAG
E
Intensity of active Bax
150
100
50
0
*
DMSO
5uM etoposide
2
4
Time (hours)
F
3xFLAG-TRIM17
VEC
WT
C16A
Etop: – + – + – +
FLAG
β-actin

Figure 6. Proteomic screen (I) to identify interacting partners of TRIM17. A. Screen workflow. The screen was carried out in HEK293 Flp-In Trex cells overexpressing WT or C16A mutant 3xFLAG-TRIM17. B. Western blot showing equal induction of WT and C16A TRIM17 after both 24 and 40 hr of tetracycline treatment. C. Western blot showing tetracycline titration to optimize induction of both WT and C16A. D. Western blot showing FLAG-specificity of immunoprecipitation (IP) of 3xFLAG-TRIM17 (WT shown here). E. Histogram showing quantification of 6A7 fluorescent intensity in 293 Flp-In Trex cells following 2 and 4 hr etoposide (5 uM) treatment (*$p < 0.01$). F. Western blot showing equal protein (β-actin) in control and 2 hr etoposide-treated (5 uM) samples.

beads was confirmed by incubating 293 cell lysates with Protein A/G beads in parallel (Figure 6D). With a view of identifying an interacting partner of WT Trim17 that is specifically found in cells undergoing the early stages of apoptosis, the time required for Bax activation in HEK293 cells after etoposide treatment was determined (Figure 6E). After 2 hours of etoposide treatment there was a ~2-fold increase in the fluorescent intensity of 6A7 (active Bax). Finally, to confirm that the etoposide treatment was not too severe and allowing for the later stages of cell death at the 2-hour time point, the protein levels of 3xFLAG-Trim17 and β-actin were verified by WB analysis (Figure 6F). The etoposide treatment did not appear to decrease the levels of either protein.

The MS analysis from this screen did not identify any binding partners specific to WT Trim17. A high degree of background was observed with this method, meaning many hits identified in the Trim17 samples were also present in the vector-only control sample (list of top 98 hits – Appendix B). Notably, there was a 2-fold increase over vector control in the number of tubulin peptides that were found in both the WT and C16A samples, suggesting that Trim17 may form a complex with tubulin in HEK293 cells.

3.4.2 Proteomic approach II: Recombinant GST-RING-TRIM17 pulldown from mouse brain lysates

The second approach taken to identify Trim17 interacting partners was a pulldown from mouse brain lysates using the recombinant, GST-tagged RING domain of Trim17 or a GST-only control (Figure 7A). The RING domain was chosen

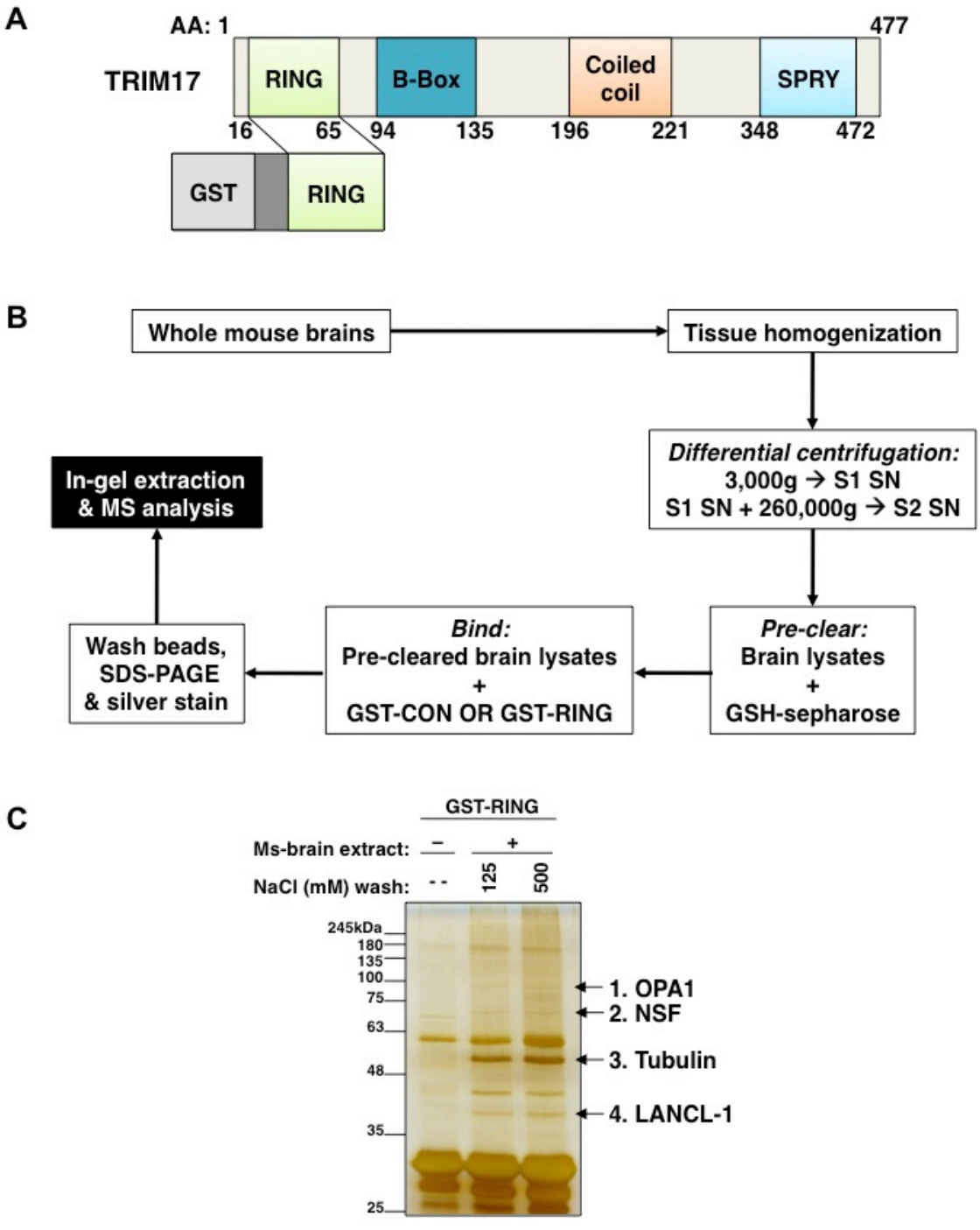
A
AA: 1
477
TRIM17
RING
B-Box
Coiled coil
SPRY
16
65
94
135
196
221
348
472
GST
RING
B
Whole mouse brains
Tissue homogenization
Differential centrifugation:
3,000g → S1 SN
S1 SN + 260,000g → S2 SN
In-gel extraction & MS analysis
Pre-clear:
Brain lysates
+
GSH-sepharose
Bind:
Pre-cleared brain lysates
+
GST-CON OR GST-RING
Wash beads, SDS-PAGE & silver stain
C
GST-RING
Ms-brain extract: – +
NaCl (mM) wash: - - 125 500
245kDa
180
135
100
75
63
48
35
25
1. OPA1
2. NSF
3. Tubulin
4. LANCL-1

Figure 7. Proteomic screen (II) to identify interacting partners of the RING domain of TRIM17. A. Schematic depicting recombinant GST-RING-TRIM17. B. Screen workflow. C. Silver-stained gel showing pulldown of potential interacting partners from mouse brain extracts using GST-RING bait. Bands unique to TRIM17 are marked with arrows. The bands were analyzed by mass spectrometry and identified to be (1) OPA1, (2) NSF, (3) tubulin & (4) LANCL-1.

as it has been shown to confer its E3 ubiquitin ligase activity and is required for its pro-apoptotic effect in CGNs [114, 118, 119]. Mouse brain lysates were incubated with the GST-RING protein and resolved by SDS-PAGE. Four silver-stained gel bands that appeared to be specific to the GST-RING with lysate sample were cut and analyzed by MS (Figure 7B). These bands were determined to be optic atrophy 1 (Opa1), N-ethylmaleimide sensitive fusion protein (NSF), tubulin and LanC lantibiotic synthetase component C-like 1 (Lancl-1) (Figure 7C, full gel with GST-control – Appendix C, MS data – Appendix D). The complex formation of GST-RING-Trim17 with NSF, Opa1 and tubulin were each confirmed by WB (Figure 8A, Appendix E).

3.5 Trim17 forms a complex with Opa1 and facilitates its degradation

The disruption of Opa1 complexes at cristae junctions is known to occur during apoptosis [85, 88]. This led me to consider whether Trim17 facilitates cell death by down-regulating Opa1 levels and subsequently disrupting cristae junctions. Trim17 was previously reported to be a cytoplasmic protein based on the overexpression of a GFP-tagged construct [112], however Opa1 is localized to the inner membrane and matrix of mitochondria [81]. In order to investigate the likelihood of an Opa1-Trim17 complex in cells, cortical neurons were separated into cytosolic and heavy membrane fractions. Western blot analysis showed a significant amount of endogenous Trim17 in both the cytosolic and heavy membrane (mitochondrial-containing) fractions (Figure 8B). Opa1 was enriched in the membrane fraction. These data show that Trim17 and Opa1 can exist together in

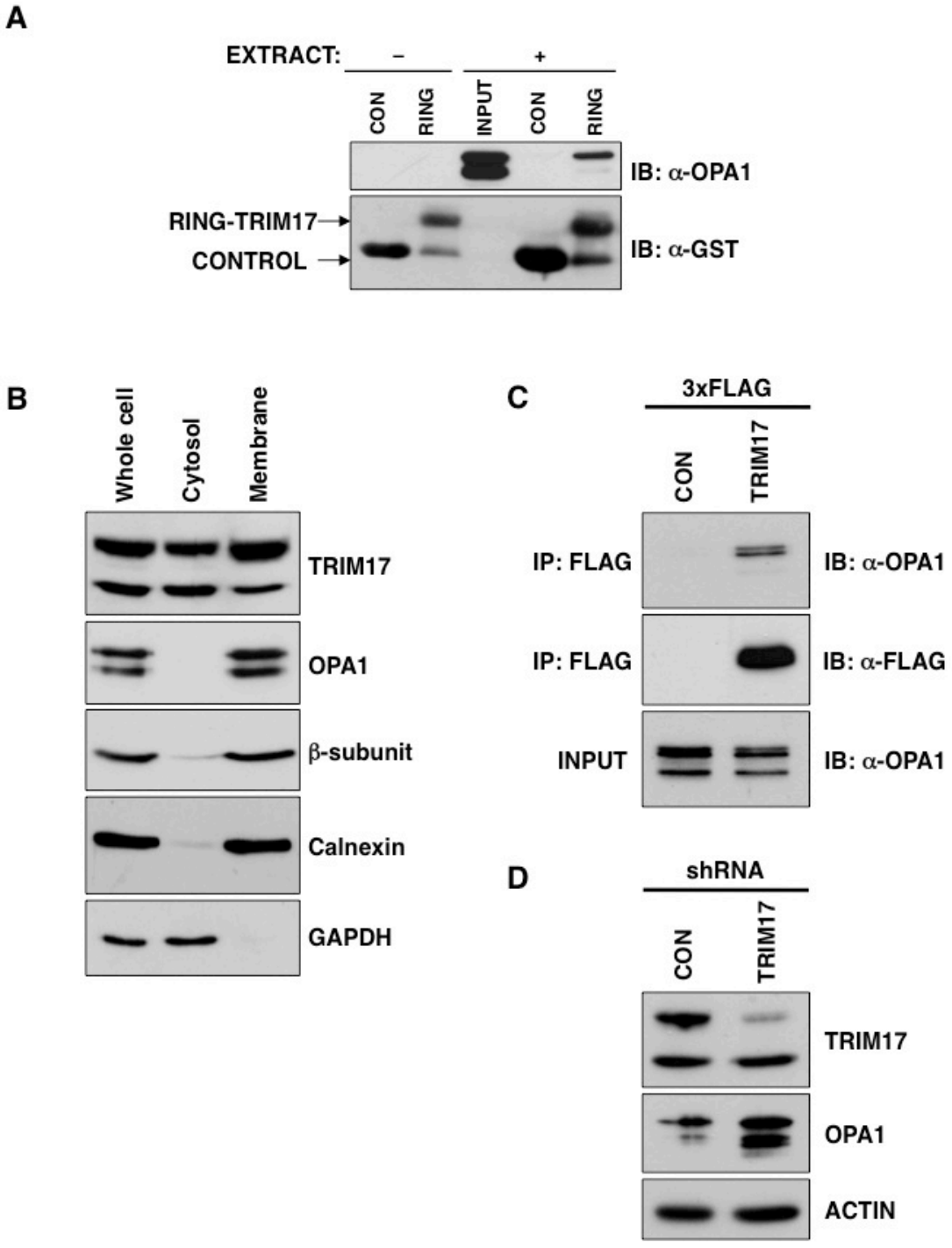
A
EXTRACT:
–
+
CON
RING
INPUT
CON
RING
IB: α-OPA1
RING-TRIM17
CONTROL
IB: α-GST
B
Whole cell
Cytosol
Membrane
TRIM17
OPA1
β-subunit
Calnexin
GAPDH
C
3xFLAG
CON
TRIM17
IP: FLAG
IB: α-OPA1
IP: FLAG
IB: α-FLAG
INPUT
IB: α-OPA1
D
shRNA
CON
TRIM17
TRIM17
OPA1
ACTIN

Figure 8. TRIM17 forms a complex with and regulates OPA1. A. Western blot confirming that GST-RING-TRIM17 forms a complex with OPA1 in mouse brain extracts. B. Endogenous TRIM17 is found in both the cytosol and heavy-membrane fractions of cortical neurons under steady-state conditions. OPA1 enrichment in the membrane fraction is shown. β-subunit (mitochondria), calnexin (ER) and GAPDH (cytosol) loading controls are shown. C. Western blot showing co-immunoprecipitation of OPA1 specifically with WT 3xFLAG-TRIM17, as compared to the vector control (CON), from HEK293 TRex cells. Input sample is representative of 1% of total lysate. D. Western blot showing OPA1 levels in TRIM17 knockdown neuronal cultures.

the same subcellular compartment in neurons and provide further support the possibility of a direct interaction.

To determine if endogenous Opa1 forms a complex with exogenous Trim17 in cells, I used HEK293 TRex cells stably expressing the vector-only control or the WT 3xFLAG-Trim17, and observed that Opa1 co-immunoprecipitated with 3xFLAG-Trim17 (Figure 8C).

In order to examine the biological relevance of an Opa1-Trim17 complex in neurons, the effect of Trim17 knockdown on Opa1 protein levels was assessed. WB analysis showed that, under steady-state conditions, Trim17 knockdown cells had a significantly higher level of Opa1 (Figure 8D).

Chapter 4: Discussion

The intrinsic pathway of apoptosis has been shown to be upregulated following ischemic injury. The initiation of this pathway gives rise to the signaling cascade that causes MOMP, caspase activation and eventually neuronal cell death. The inhibition of factors downstream of MOMP (AIF, caspases) has been found to reduce the level of cell loss in experimental models. However, the therapeutic potential of these downstream targets in stroke has been limited due to a variety of reasons [129, 130]. In addition, the inhibition of factors downstream of MOMP alone does not prevent the mitochondrial dysfunction associated with apoptosis. This results in ATP-depletion due to a lack of oxidative phosphorylation and promotes a necrotic type of death in neurons [131, 132]. The central role of tBid in this process, and its association with Bax activation, makes the identification of events upstream of MOMP particularly attractive from a therapeutic point of view.

I have shown that knockdown of Trim17 delays tBid-induced death in cortical neurons. These data are consistent with past work from Lassot et al., identifying a role for Trim17 during apoptosis in CGNs [118]. The results presented here in cortical neurons have added significance in the context of stroke as the majority of ischemic injuries occur in the cerebral cortex of the brain, rather than the cerebellum (CGNs) [135, 136]. Additionally, the choice of tBid as a pro-death stimulus in the work shown here circumvents the requirement of the caspase 8 cleavage of Bid. Through the use of this focused stimulus it can be inferred that Trim17 acts downstream of Bid activation. The role of Trim17 in a more physiologically relevant experimental model of stroke warrants investigation. Ongoing work aimed at

characterizing the effect of the loss of Trim17 on OGD-induced death in cortical neurons will provide insight on this topic.

As described in detail in earlier chapters, past studies have shown that tBid facilitates the Bax activation step that is followed by MOMP, loss of membrane potential and a reduction in oxidative phosphorylation [16]. I have shown here that downregulation of Trim17 in the presence of tBid delays these post-MOMP effects in cortical neurons. Trim17 knockdown cultures maintained mitochondrial membrane potential after tBid-treatment. This implies that knockdown neurons are able to maintain the functional electron transport required for generating membrane potential. Consistent with this, Trim17 knockdown cells were found to better maintain maximal respiratory capacity in the presence of tBid. These cells also maintained higher ATP levels under this same apoptotic stress. These data, taken together with the maintenance of electron transport and preservation of ATP levels, suggest that neurons with reduced Trim17 expression are able to continue oxidative phosphorylation in the presence of tBid.

The inhibition of caspases to block apoptotic death can promote a necrotic form of death in the context of a neuron because of this cell type's elevated energy demands. The observation that knockdown of Trim17 not only delays death in cortical neurons, but also maintains mitochondrial function and ATP synthesis in the presence of tBid, is especially attractive from a therapeutic point of view for ischemic injury. Mechanistically, these observations provide convincing evidence that Trim17 acts upstream of MOMP during cell death. Given the data from the initial pilot screens suggesting that Trim17 promotes Bax activation, the effect of Trim17

specifically on this process as well as Bax oligomerization in cortical neurons still needs to be determined. This will aid in the precise positioning of Trim17 in the intrinsic pathway.

Trim17 has been shown to possess E3 ubiquitin ligase activity. At the time of this work only two interacting partners, Trim44 and ZWINT, had been proposed [114, 118]. Using an unbiased proteomic approach, I successfully identified Opa1, Nsf and tubulin as forming complexes with the RING domain of Trim17 in mouse brain extracts. Lancl-1 was not validated due to the lack of commercially available antibodies. Tubulin was not pursued as a hit because of two main reasons. The first reason being that the relative abundance of cytoskeletal proteins in the extracts may provide a bias to the identification of these types of interactions. Secondly, initial experiments suggested no effect of knocking down Trim17 on tubulin morphology under steady-state conditions (Appendix E). Still, these data cannot completely rule of the possibility of a real tubulin-Trim17 interaction in cells, as there have been ubiquitinated forms of tubulin found in rat brain lysates. Another E3-ligase, Parkin, has been shown to ubiquitinate tubulin *in vitro*, however implications of such an interaction *in vivo* remain to be completely characterized [139].

The potential interaction of Trim17 with Nsf may have important biological consequences. Preliminary work has shown that loss of Trim17 in cortical neurons produces an downregulation of Nsf protein levels, contrary to what may be expected for an E3 that targets substrates for proteosomal degradation (data not shown). This could be suggestive of an indirect Nsf-Trim17 interaction that remains to be

characterized in future work. Nsf is an ATPase involved in membrane fusion and is a central component of the SNARE (Soluble Nsf Attachment Protein Receptor) complex [140]. Recent evidence for the interaction of RING-finger protein RNF13 with snapnin, a protein that primarily interacts with SNAP-25 (another member of the SNARE complex), has emerged [141]. Genetic ablation of RNF13 in mice impaired SNARE complex assembly within the hippocampus and had a negative effect on spatial learning by the Morris water maze test. The prospect of multiple regulatory mechanisms of the SNARE complex mediated by RING-containing E3's provides further support for the investigation of an Nsf-Trim17 interaction in neurons.

From the list of proteomic hits, I chose to focus on Opa1 because of its well-characterized role in the intrinsic pathway. I was therefore interested in determining the potential mechanism by which an Opa1-Trim17 interaction may facilitate cell death. In order to first determine the feasibility of this interaction, I determined the subcellular localization of endogenous Trim17 in cortical neurons. Trim17 was enriched in both the cytosolic and heavy-membrane fractions whereas Opa1 was exclusively located in the membrane fraction. These findings support the notion that Trim17 could interact with Opa1 in mitochondria. Moreover, endogenous Opa1 was found to co-immunoprecipitate with exogenously expressed Trim17 in cells. Co-immunoprecipitation of the two endogenous proteins remains to be done in neurons, but these data show that Opa1 forms a complex with not only the RING-domain but also full-length Trim17.

The biological relevance of a potential Opa1-Trim17 interaction was investigated. Loss of Trim17 in cortical neurons was found to give an upregulation

of Opa1 protein levels under steady-state conditions. This suggests that the E3-ligase activity of Trim17 negatively regulates Opa1 levels in cells. Whether this regulation is through the direct ubiquitination of Opa1 by Trim17 remains to be determined. Chronic inhibition of mitochondrial fission with 15d-PGJ2 (15-deoxy-Δ 12,14-prostaglandin J2), a Drp1 inhibitor, has been shown to cause mitochondrial swelling and irregular cristae structures in rat kidney proximal tubule cells (RPTC). These changes in mitochondrial morphology were reported to be accompanied by decreased Opa1 levels as well as the ubiquitination of newly synthesized Opa1 [142]. Moreover, efforts to systematically characterize the ubiquitin-modified proteome have identified two peptide motifs within Opa1 that are ubiquitinated [143]. These data therefore provide additional support for a model whereby Opa1 can be targeted for proteasomal degradation.

During apoptosis Opa1 complexes that serve to maintain cristae junctions are dismantled in order to release cytochrome *c* from mitochondria. This occurs in a Bax/Bak-dependent manner following MOMP [87]. While the downregulation of Opa1 sensitizes cells to death, overexpression of Opa1 has been shown to confer protection against excitotoxic stress in CGNs [81, 144]. Knockdown of Trim17 was found to increase Opa1 levels, suggesting that Trim17 is required for Opa1 turnover. The data shown here also suggest that knockdown of Trim17 phenocopies Opa1 overexpression, thereby conferring resistance to tBid-induced apoptosis in cortical neurons. This gives rise to a simple model in cortical neurons whereby upregulation

1. CYTOSOLIC TRIM17

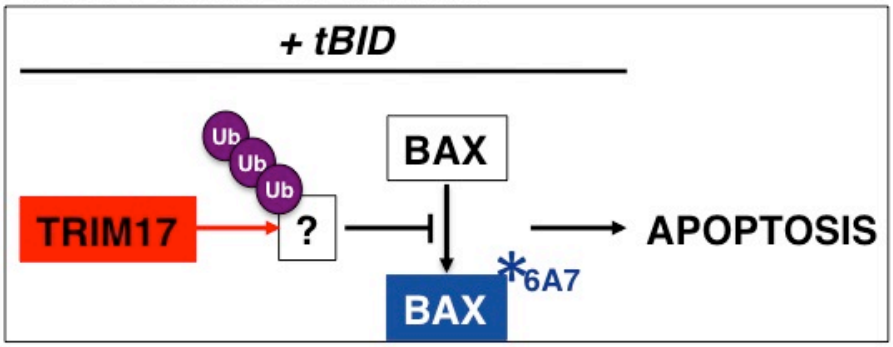

2. MITOCHONDRIAL TRIM17

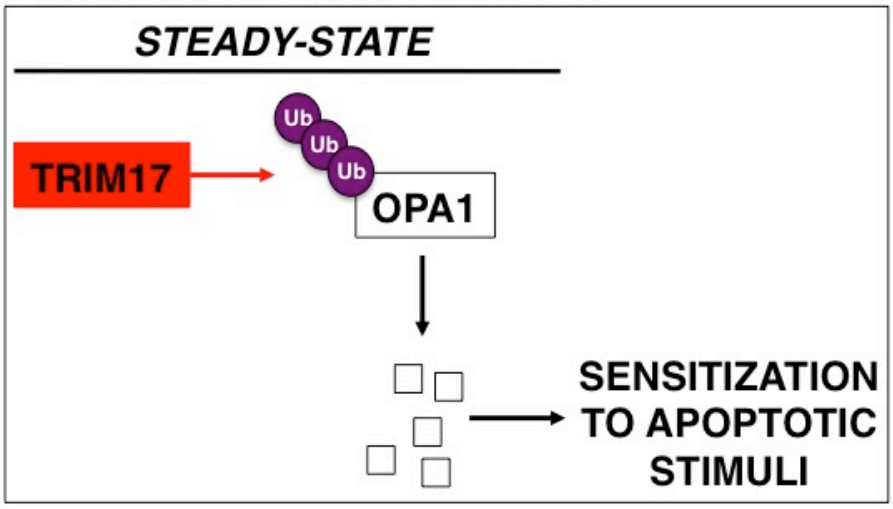

Figure 9. Proposed model for the regulation of BAX-dependent apoptosis by TRIM17 at two separate points. (1) Cytosolic TRIM17 ubiquitinates a repressor of BAX activation. (2) Mitochondrial TRIM17 ubiquitinates OPA1, leading to its proteosomal degradation, widening of cristae junctions, and sensitization to apoptotic stimuli.

of Opa1 under steady-state conditions, through the reduction of Trim17 E3-ligase activity, delays the dismantling of Opa1-cristae structures upon apoptotic stress (Figure 9). Preliminary data shows that, with the initiation of apoptosis, Opa1 levels begin to decrease as early as 4 hours after tBid-treatment in cortical neurons (data not shown). Ongoing studies looking at the kinetics of tBid-induced Opa1 downregulation in the presence or absence of Trim17 will help to determine if this potential interaction is also relevant in an apoptotic setting.

The Trim17-mediated regulation of another anti-apoptotic protein has very recently (September 2012) been proposed to occur in CGNs. Previous studies have shown that the proteolytic degradation of myeloid-cell leukemia 1 (Mcl-1) is required for the initiation of apoptosis in several cell lines [145-147]. The degradation of Mcl-1 was also found to be dependent on GSK3 activity [146]. Now it has been shown that Trim17 co-immunoprecipitates with Mcl-1 from neuroblastoma cells and that it can ubiquitinate Mcl-1 *in vitro*. In terms of function, knockdown of Trim17 was found to increase total Mcl-1 protein levels while decreasing the levels of ubiquitinated Mcl-1 in CGNs. Conversely, overexpression of Trim17 decreased Mcl-1 levels in a manner that was dependent on GSK3 activity [148]. These data are very interesting in light of the recent discovery that Mcl-1 is not only an OMM protein as traditionally thought, but is actually proteolytically processed and imported into mitochondria [149]. However, the anti-apoptotic functions of Mcl-1 are thought to reside in the long isoform that remains on the OMM. The truncated isoform of Mcl-1 is imported into the mitochondrial matrix where it participates in a variety of activities including respiration, ATP production, and the maintenance of cristae ultrastructure. Further

characterization of exactly which isoform of Mcl-1 is ubiquitinated by Trim17 is required. This will aid in determining whether the complex formation of Trim17 with Opa1 is a separate entity or whether it has been identified because the short isoform of Mcl-1 exists in close proximity to Opa1 within the mitochondrial matrix. Then again, it is important to note that a Mcl-1-Opa1 complex has yet to be identified.

The mechanism by which Trim17 protects neurons against death may occur at different steps in the intrinsic pathway. The initial data from the genetic screens for regulators of Bax activation suggested a role for Trim17 at this step in the process. However, the identification of Opa1 as being a member of a Trim17 protein complex in cells makes it an attractive explanation for why neuronal cell death is delayed in the absence of this E3 ligase. The possibility of multiple regulatory roles for Trim17 is especially appealing in light of the recent data showing that Mcl-1 is a Trim17 substrate. Mcl-1 is known to heterodimerize with Bax to inhibit apoptosis [150, 151]. It is possible that cytosolic Trim17 targets OMM-Mcl-1 for degradation while mitochondrial Trim17 downregulates the level of Opa1. The combination of these two actions would lead to cells being more “primed” for death compared to cells in which Trim17 is absent. Therefore it may be possible that Trim17 exerts two distinct pro-apoptotic effects by downregulating the levels of both Mcl-1 and Opa1.

Conclusion

I propose that Trim17 forms a complex with and promotes the turnover of Opa1 within the mitochondrial matrix under steady-state conditions (Figure 9). In the absence of this regulation (i.e. Trim17 knockdown) cells accumulate higher levels of Opa1 and are better capable to maintain cristae junctions and mitochondrial function in the presence of an apoptotic stimulus. This ultimately leads to a delay, but not complete block, in neuronal cell death.

References

1. Kerr, J.F., A.H. Wyllie, and A.R. Currie, *Apoptosis: a basic biological phenomenon with wide-ranging implications in tissue kinetics.* Br J Cancer, 1972. **26**(4): p. 239-57.
2. Fadok, V.A., Voel, D.R., Campbell, P.A., Cohen, J.J., Bratton, D.L., Henson, P.M., *Exposure of phosphatidylserine on the surface of apoptotic lymphocytes triggers specific recognition and removal by macrophages.* J Immunol., 1992. **148**(7): p. 2207-2216.
3. Fink, S.L., Cookson, B.T., *Apoptosis, Pyroptosis, and Necrosis: Mechanistic Description of Dead and Dying Eukaryotic Cells.* Infect. Immun., 2005. **73**(4): p. 1907-1916.
4. Ashkenzi, A., *Targeting death and decoy receptors of the tumor-necrosis factor superfamily.* Nat. Rev. Cancer, 2002. **2**(6): p. 420-430.
5. Green, D.R., Reed, J.C., *Mitochondria and Apoptosis: .* Science, 1998. **281**(5381): p. 1309-1312.
6. Thornberry, N.A., Lazebnik, Y., *Caspases: Enemies within.* Science, 1998. **281**(5381): p. 1312-1316.
7. Shi, Y., *Mechanisms of caspase activation and inhibition during apoptosis.* Mol Cell, 2002. **9**(3): p. 459-470.
8. Yin, X.M., Wang, K., Gross, A., Zhao, Y., Zinkel, S., Klocke, B., Roth, K.A., Korsmeyer, S.J., *Bid-deficient mice are resistant to Fas-induced hepatocellular apoptosis.* Nature, 1999. **400**(6747): p. 886-891.
9. Yuan, J., Yankner, B.A., *Apoptosis in the nervous system.* Nature, 2000. **407**(6805): p. 802-809.
10. Mattson, M.P., M. Gleichmann, and A. Cheng, *Mitochondria in neuroplasticity and neurological disorders.* Neuron, 2008. **60**(5): p. 748-66.
11. Thompson, C.B., *Apoptosis in the pathogenesis and treatment of disease.* Science, 1995. **267**(5203): p. 1456-1462.
12. Gottlieb, E., Armour, S.M., Harris, M.H., Thompson, C.B., *Mitochondrial membrane potential regulates matrix configuration and cytochrome c release during apoptosis.* Cell Death and Differentiation, 2003. **10**: p. 709-717.
13. Liu, X., Kim, CN., Yang, J., Jemmerson, R., Wang, X., *Induction of apoptotic program in cell-free extracts: requirement for dATP and cytochrome c.* Cell, 1996. **86**(1): p. 147-157.
14. Zou, H., Henzel, W.J., Liu, X., Lutschg, A., Wang, X., *Apaf-1, a human protein homologous to C. elegans CED-4, participates in cytochrome c-dependent activation of caspase-3.* Cell, 1997. **90**(3): p. 405-413.
15. Zou, H., Li, Y., Liu, X., Wang, X., *An APAF-1, cytochrome c multimeric complex is a functional apoptosome that activates procaspase-9.* J Biol Chem, 1999. **274**(17): p. 11549-11556.
16. Tait, S.W. and D.R. Green, *Mitochondria and cell death: outer membrane permeabilization and beyond.* Nat Rev Mol Cell Biol, 2010. **11**(9): p. 621-32.

17. Li, L.Y., Luo, X., Wang, X., *Endonuclease G is an apoptotic DNase when released from mitochondria.* Nature, 2001. **412**(6842): p. 95-99.
18. Joza, N., Susin, S.A., Daugas, E., Stanford, W.L., Cho, S.K., Li, C.Y., Sasaki, T., Elisa, A.J., Cheng, H.Y., Ravagnan, L., Ferri, K.F., Zamzami, N., Wakeham, A., Hakem, R., Yoshida, H., Kong, Y.Y., Mak, T.W., Zuniga-Pflucker, J.C., Kroemer, G., Penninger, J.M., *Essential role of the mitochondrial apoptosis-inducing factor in programmed cell death.* Nature, 2001. **410**(6828): p. 549-554.
19. Wei, M.C., Zong, W.X., Cheng, E.H., Lindsten, T., Panoutsakopoulou, V., Ross, A.J., Roth, K.A., MacGregor, G.R., Thompson, C.B., Korsmeyer, S.J., *Proapoptotic Bax and Bak: a requisite gateway to mitochondrial dysfunction and death.* Science, 2001. **292**(5517): p. 727-730.
20. Eskes, R., Desagher, S., Antonsson, B., Martinou, J.C., *Bid induces the oligomerization and insertion of Bax into the outer mitochondrial membrane.* Mol Cell Biol, 2000. **20**(3): p. 929-935.
21. Wei, M.C., Lindsten, T., Mootha, V.K., Weiler, S., Gross, A., Ashiya, M., Thompson, C.B., Korsmeyer, S.J., *tBID, a membrane-targeted death ligand, oligomerizes BAK to release cytochrome c.* Genes Dev, 2000. **14**(16): p. 2060-2071.
22. Wolter, K.G., Hsu, Y.T., Smith, C.L., Nechushtan, A., Xi, X.G., Youle, R.J., *Movement of Bax from the cytosol to mitochondria during apoptosis.* J Cell Biol, 1997. **139**(5): p. 1281-1292.
23. Hsu, Y.T., Youle, R.J., *Nonionic detergents induce dimerization among members of the Bcl-2 family.* J Biol Chem, 1997. **272**(21): p. 13829-13834.
24. Hsu, Y.T., Youle, R.J., *Bax in murine thymus is a soluble monomeric protein that displays differential detergent-induced conformations.* J Biol Chem, 1998. **273**(17): p. 10777-10783.
25. Yethon, J.A., Epand, R.F., Leber, B., Epand, R.M., Andrews, D.W., *Interaction with a membrane surface triggers a reversible conformational change in Bax normally associated with induction of apoptosis.* J Biol Chem, 2003. **278**(49): p. 48935-48941.
26. George, N.M., Evans, J.J., Luo, X., *A three-helix homo-oligomerization domain containing BH3 and BH1 is responsible for the apoptotic activity of Bax.* Genes Dev, 2007. **21**(15): p. 1937-1948.
27. Dewson, G., Kratina, T., Sim, H.W., Puthalakath, H., Adams, J.M., Colman, P.M., Kluck, R.M., *To trigger apoptosis, Bak exposes its BH3 domain and homodimerizes via BH3:groove interactions.* Mol Cell, 2008. **30**(3): p. 369-380.
28. Lovell, J.F., Billen, L.P., Bindner, S., Shamas-Din, A., Fradin, C., Leber, B., Andrews, D.W., *Membrane binding by tBid initiates an ordered series of events culminating in membrane permeabilization by Bax.* Cell, 2008. **135**(6): p. 1074-1084.
29. Zaltsman, Y., Shachnai, L., Yivgi-Ohana, N., Schwarz, M., Maryanovich, M., Houtkooper, R.H., Vaz, F.M., De Leonardis, F., Fiermonte, G., Palmieri, F., Gillissen, B., Daniel, P.T., Jimenez, E., Walsh, S., Koehler, C.M., Roy, S.S.,

Water, L., Hajnoczky, G., Gross, A., *MTCH2/MIMP is a major facilitator of tBID recruitment to mitochondria.* Nat Cell Biol, 2010. **12**(6): p. 553-562.
30. Zamzami, N., Kroemer, G., *The mitochondrion in apoptosis: how Pandora's box opens.* Nat Rev Mol Cell Biol, 2001. **2**(1): p. 67-71.
31. Green, D.R., Kroemer, G., *The pathophysiology of mitochondrial cell death.* Science, 2004. **305**(5684): p. 626-629.
32. Eskes, R., Antonsson, B., Osen-Sand, A., Montessuit, S., Richter, C., Sadoul, R., Mazzei, G., Nichols, A., Martinou, J.C., *Bax-induced cytochrome c release from mitochondria is independent of the permeability transition pore but highly dependent on Mg2+ ions.* J Cell Biol, 1998. **143**(1): p. 217-224.
33. Kokoszka, J.E., Waymire, K.G., Levy, S.E., Sligh, J.E., Cai, J., Jones, D.P., MacGregor, G.R., Wallace, D.C., *The ADP/ATP translocator is not essential for the mitochondrial permeability transition pore.* Nature, 2004. **427**(6973): p. 461-465.
34. Baines, C.P., Kaiser, R.A., Purcell, N.H., Blair, N.S., Osinska, H., Hambleton, M.A., Brunskill, E.W., Sayen, M.R., Gottlieb R.A., Dorn, G.W., Robbins, J., Molkentin, J.D., *Loss of cyclophilin D reveals a critical role for mitochondrial permeability transition in cell death.* Nature, 2005. **434**(7033): p. 658-662.
35. Nakagawa, T., Shimizu, S., Watanabe, T., Yamaguchi, O., Otsu, K., Yamagata, H., Inohara, H., Kubo, T., Tsujimoto, Y., *Cyclophilin D-dependent mitochondrial permeability transition regulates some necrotic but not apoptotic cell death.* Nature, 2005. **434**(7033): p. 652-658.
36. Shimizu, S., Narita, M., Tsujimoto, Y., *Bcl-2 family proteins regulate the release of apoptogenic cytochrome c by the mitochondrial channel VDAC.* Nature, 1999. **399**(6735): p. 483-487.
37. Shimizu, S., Ide, T., Yanagida, T., Tsujimoto, Y., *Electrophysiological study of a novel large pore formed by Bax and the voltage-dependent anion channel that is permeable to cytochrome c.* J Biol Chem, 2000. **275**(16): p. 12321-12325.
38. Shimizu, S., Konishi, A., Kodama, T., Tsujimoto, Y., *BH4 domain of antiapoptotic Bcl-2 family members closes voltage-dependent anion channel and inhibits apoptotic mitochondrial changes and cell death.* Proc Natl Acad Sci, 2000. **97**(7): p. 3100-3105.
39. Rostovtseva, T.K., Antonsson, B., Suzuki, M., Youle, R.J., Colombini, M., Bezrukov, S.M., *Bid, but not Bax, regulates VDAC channels.* J Biol Chem, 2004. **279**(14): p. 13575-13583.
40. Baines, C.P., Kaiser, R.A., Sheiko, T., Craigen, W.J., Molkentin, J.D., *Voltage-dependent anion channels are dispensable for mitochondrial-dependent cell death.* Nat Cell Biol, 2007. **9**(5): p. 550-555.
41. Annis, M.G., Soucie, E.L., Dlugosz, P.J., Cruz-Aguado, J.A., Penn, L.Z., Leber, B., Andrews, D.W., *Bax forms multispanning monomers that oligomerize to permeabilize membranes during apoptosis.* The EMBO Journal, 2005. **24**(2096-2103).

42. Dewson, G., Kratina, T., Czabotar, P., Day, C.L., Adams, J.M., Kluck, R.M., *Bak activation for apoptosis involves oligomerization of dimers via their alpha6 helices.* Mol Cell, 2009. **36**(4): p. 696-703.
43. Suzuki, M., Youle, R.J., Tjandra, N., *Structure of Bax: coregulation of dimer formation and intracellular localization.* Cell, 2000. **103**(4): p. 645-654.
44. Hardwick, J.M., Polster, B.M., *Bax, along with lipid conspirators, allows cytochrome c to escape mitochondria.* Mol Cell, 2002. **10**(5): p. 963-965.
45. Basanez, G., Nechushtan, A., Drozhini, O., Chanturiya, A., Choe, E., Tutt, S., Wood, K.A., Hsu, Y.T., Zimmerberg, J., Youle, R.J., *Bax, but not Bcl-XL, decreases the lifetime of planar phospholipid bilayer membranes at subnanomolar concentrations.* Proc Natl Acad Sci, 1999. **96**(10): p. 5492-5497.
46. Oda, E., Ohki, R., Murasawa, H., Nemoto, J., Shibue, T., Yamashita, T., Tokino, T., Taniguchi, T., Tanaka, N., *Noxa, a BH3-only member of the Bcl-2 family and candidate mediator of p53-induced apoptosis.* Science, 2000. **288**(5468): p. 1053-1058.
47. Dijkers, P.F., Medema, R.H., Lammers, J.W., Koenderman, L., Coffer, P.J., *Expression of the pro-apoptotic Bcl-2 family member Bim is regulated by the forkhead transcription factor FKHR-L1.* Curr Biol, 2000. **10**(19): p. 1201-1204.
48. Sax, J.K., Fei, P., Murphy, M.E., Bernhard, E., Korsmeyer, S.J., El-Deiry, W.S., *BID regulation by p53 contributes to chemosensitivity.* Nat Cell Biol, 2002. **4**(11): p. 842-849.
49. Miyashita, T., Krajewski, S., Krajewski, M., Wang, H.G., Lin, H.K., Liebermann, D.A., Hoffman, B., Reed, J.C., *Tumor suppressor p53 is a regulator of bcl-2 and bax gene expression in vitro and in vivo.* Oncogene, 1994. **9**(6): p. 1799-1805.
50. Grad, J.M., Zeng, X.R., Boise, L.H., *Regulation of Bcl-XL: a little bit of this and a little bit of STAT.* Curr Opin Oncol., 2000. **12**(6): p. 543-549.
51. Youle, R.J., Strasser, A., *The Bcl-2 protein family: opposing activites that mediate cell death.* Nat Rev Mol Cell Biol, 2008. **9**(1): p. 47-59.
52. Green, D.R., *At the gates of death.* Cancer Cell, 2006. **9**(5): p. 328-330.
53. Uren, R.T., Dewson, G., Chen, L., Coyne, S.C., Huang, D.C., Adams, J.M., Kluck, R.M., *Mitochondrial permeabilization relies on BH3 ligands engaging multiple prosurvival Bcl-2 relatives, not Bak.* J Cell Biol, 2007. **177**(2): p. 277-287.
54. Willis, S.N., Fletcher, J.I., Kaufmann, T., van Delft, M.F., Chen, L., Czabotar, P.E., Ierino, H., Lee, E.F., Fairlie, W.D., Bouillet, P., Strasser, A., Kluck, R.M., Adams, J.M., Huang, D.C., *Apoptosis initiated when BH3 ligands engage multiple Bcl-2 homologs, not Bax or Bak.* Science, 2007. **315**(5813): p. 856-859.
55. Kim, H., Rafluddin-Shah, M., Tu, H.C., Jeffers, J.R., Zambetti, G.P., Hsieh, J.J., Cheng, E.H., *Hierarchical regulation of mitochondrion-dependent apoptosis by Bcl-2 subfamilies.* Nat Cell Biol, 2006. **8**(12): p. 1348-1358.
56. Certo, M., Del Gaizo Moore, V., Nishino, M., Wei, G., Korsmeyer, S., Armstrong, S.A., Letai, A., *Mitochondria primed by death signals determine*

cellular addiction to antiapoptotic Bcl-2 family members. Cancer Cell, 2006. **9**(5): p. 351-365.
57. Letai, A., Bassik, M.C., Walensky, L.D., Sorcinelli, M.D., Weiler, S., Korsmeyer, S.J., *Distinct BH3 domains either sensitize or activate mitochondrial apoptosis, serving as prototype cancer therapeutics.* Cancer Cell, 2002. **2**(3): p. 183-192.
58. Billen, L.P., Kokoski, C.L., Lovell, J.F., Leber, B., Andrews, D.W., *Bcl-XL inhibits membrane permeabilization by competing with Bax.* PLoS, 2008. **6**(6): p. 1268-1280.
59. Merino, D., Glam, M., Hughes, P.D., Siggs, O.M., Heger, K., O'Reilly, L.A., Adams, J.M., Strasser, A., Lee, E.F., Fairlie, W.D., Bouillet, P., *The role of BH3-only Bim extends beyond inhibiting Bcl-2-like prosurvival proteins.* J Cell Biol, 2009. **186**(3): p. 355-362.
60. Chipuk, J.E., Green, D.R., *How do Bcl-2 proteins induce mitochondrial outer membrane permeabilization?* Trends in Cell Biology, 2008. **18**(4): p. 157-164.
61. Villunger, A., Labi, V., Bouillet, P., Adams, J., Strasser, A., *Can the analysis of BH3-only protein knockout mice clarify the issue of 'direct versus indirect' activation of Bax and Bak?* Cell Death Differ., 2011. **18**(10): p. 1545-1546.
62. Llambi, F., Moldoveanu, T., Tait, S.W., Bouchier-Hayes, L., Temirov, J., McCormick, L.L., Dillon, C.P., Green, D.R., *A unified model of mammalian BCL-2 protein family interactions at the mitochondria.* Mol Cell, 2011. **44**(4): p. 517-531.
63. Chen, L., Willis, S.N., Wei, A., Smith, B.J., Fletcher, J.I., Hinds, M.G., Colman, P.M., Day, C.L., Adams, J.M., Huang, D.C., *Differential targeting of prosurvival Bcl-2 proteins by their BH3-only ligands allows complementary apoptotic function.* Mol Cell, 2005. **17**(3): p. 393-403.
64. Walensky, L.D., Pitter, K., Morash, J., Oh, K.J., Barbuto, S., Fisher, J., Smith, E., Verdine, G.L., Korsmeyer, S.J., *A stapled BID BH3 helix directly binds and activates BAX.* Mol Cell, 2006. **24**(2): p. 199-210.
65. Gavathiotis, E., Suzuki, M., Davis, M.L., Pitter, K., Bird, G.H., Katz, S.G., Tu, H.C., Kim, H., Cheng, E.H., Tjandra, N., Walensky, L.D., *BAX activation is initiated at a novel interaction site.* Nature, 2008. **455**(7216): p. 1076-1081.
66. Ren, D., Tu, H.C., Kim, H., Wang, G.X., Bean, G.R., Takeuchi, O., Jeffers, J.R., Zambetti, G.P., Hsieh, J.J., Cheng, E.H., *BID, BIM, and PUMA are essential for activation of the BAX- and BAK-dependent cell death program.* Science, 2010. **330**(6009): p. 1390-1393.
67. Kim, H., Tu, H.C., Ren, D., Takeuchi, O., Jeffers, J.R., Zambetti, G.P., Hsieh, J.J.D., Cheng, E.H.Y., *Stepwise activation of Bax and Bak by tBid, Bim, and Puma initiates mitochondrial apoptosis.* Mol Cell, 2009. **36**: p. 487-499.
68. de Brito, O.M., Scorrano, L., *Mitofusin 2 tethers endoplasmic reticulum to mitochondria.* Nature, 2008. **456**(7222): p. 605-610.
69. Chipuk, J.E., McStay, G.P., Bharti, A., Kuwana, T., Clarke, C.J., Siskind, L.J., Obeid, L.M., Green, D.R., *Sphingolipid metabolism cooperates with BAK and BAX to promote the mitochondrial pathway of apoptosis.* Cell, 2012. **148**(5): p. 988-1000.

70. Johnson, B.N., Berger, A.K., Cortese, G.P., Lavoie, M.J., *The ubiquitin E3 ligase parkin regulates the proapoptotic function of Bax.* Proc Natl Acad Sci, 2012. **109**(16): p. 6283-6288.
71. Cerveny, K.L., Tamura, Y., Zhang, Z., Jensen, R.E., Sesaki, H., *Regulation of mitochondrial fusion and division.* Trends in Cell Biology, 2007. **17**(563-569).
72. Karbowski, M., Youle, R.J., *Dynamics of mitochondrial morphology in healthy cells and during apoptosis.* Cell Death and Differentiation, 2003. **10**: p. 870-880.
73. Zhang, Y., Chan, D.C., *New insights into mitochondrial fusion.* FEBS Lett., 2007. **581**(11): p. 2168-2173.
74. Heath-Engel, H.M., Shore, G.C., *Mitochondrial membrane dynamics, cristae remodelling and apoptosis.* Biochim Biophys Acta., 2006. **1763**(5-6): p. 549-560.
75. Perfettini, J.L., Roumier, T., Kroemer, G., *Mitochondrial fusion and fission in the control of apoptosis.* Trends in Cell Biology, 2005. **15**(4): p. 179-183.
76. Karbowski, M., Lee, Y.J., Gaume, B., Jeon, S.Y., Frank, S., Nechushtan, A., Santel, A., Fuller, M., Smith, C.L., Youle, R.J., *Spatial and temporal association of Bax with mitochondrial fission sites, Drp1, and Mfn2 during apoptosis.* J Cell Biol, 2002. **159**(6): p. 931-938.
77. Hoppins, S., Edlich, F., Cleland, M.M., Banerjee, S., McCaffery, J.M., Youle, R.J., Nunnari, J., *The soluble form of Bax regulates mitochondrial fusion via MFN2 homotypic complexes.* Mol Cell, 2011. **41**(2): p. 150-160.
78. Sheridan, C., Delivani, P., Cullen, S.P., Martin, S.J., *Bax- or Bak-induced mitochondrial fission can be uncoupled from cytochrome C release.* Mol Cell, 2008. **31**(4): p. 570-585.
79. Jeong, S.Y., Seol, D.W., *The role of mitochondria in apoptosis.* BMB Rep., 2008. **41**(1): p. 11-22.
80. Frank, S., Gaume, B., Bergmann-Leitner, E.S., Leitner, W.W., Robert, E.G., Catez, F., Smith, C.L., Youle, R.J., *The role of dynamin-related protein 1, a mediator of mitochondrial fission, in apoptosis.* Dev Cell, 2001. **1**(4): p. 515-525.
81. Lee, Y.J., Jeong, S.Y., Karbowski, M., Smith, C.L., Youle, R.J., *Roles of the mammalian mitochondrial fission and fusion mediators Fis1, Drp1, and Opa1 in apoptosis.* Mol Biol Cell, 2004. **15**(11): p. 5001-5011.
82. Paumard, P., Vaillier, J., Coulary, B., Schaeffer, J., Soubannier, V., Mueller, D.M., Brethes, D., di Rago, J.P., Velours, J., *The ATP synthase is involved in generating mitochondrial cristae morphology.* EMBO J., 2002. **21**(3): p. 221-230.
83. Frezza, C., Cipolat, S., Martins de Brito, O., Micaroni, M., Beznoussenko, G.V., Rudka, T., Bartoli, D., Polishuck, R.S., Daniel, N.N., De Strooper, B., Scorrano, L., *OPA1 controls apoptotic cristae remodeling independently from mitochondrial fusion.* Cell, 2006. **126**(1): p. 177-189.
84. Delettre, C., Lenaers, G., Griffoin, J.M., Gigarel, N., Lorezno, C., Belenguer, P., Pelloquin, L., Grosgeorge, J., Turc-Carel, C., Perret, E., Astaire-Dequeker, C., Lasquellec, L., Arnaud, B., Ducommun, B., Kaplan, J., Hamel, C.P.,

Nuclear gene OPA1, encoding a mitochondrial dynamin-related protein, is mutated in dominant optic atrophy. Nat. Genet., 2000. **26**(207-210).
85. Cipolat, S., Rudka, T., Hartmann, D., Costa, V., Serneels, L., Craessaerts, K., Metzger, K., Frezza, C., Annaert, W., D'Adamio, L., Derks, C., Dejaegere, T., Pellegrini, L., D'Hooge, R., Scorrano, L., De Strooper, B., *Mitochondrial rhomboid PARL regulates cytochrome c release during apoptosis via OPA1-dependent cristae remodeling.* 126, 2006. **1**(163-175).
86. Scorrano, L., Ashiya, M., Buttle, K., Weiler, S., Oakes, S.A., Manella, C.A., Korsmeyer, S.J., *A distinct pathway remodels mitochondrial cristae and mobilizes cytochrome c during apoptosis.* Dev Cell, 2002. **2**(1): p. 55-67.
87. Yamaguchi, R., Lartigue, L., Perkins, G., Scott, R.T., Dixit, A., Kushnareva, Y., Kuwana, T., Ellisman, M.H., Newmeyer, D.D., *Opa1-mediated cristae opening is Bax/Bak and BH3 dependent, required for apoptosis, and independent of Bak oligomerization.* Mol Cell, 2008. **31**(4): p. 557-569.
88. Arnoult, D., Grodet, A., Lee, Y.J., Estaquier, J., Blackstone, C., *Release of OPA1 during apoptosis participates in the rapid and complete release of cytochrome c and subsequent mitochondrial fragmentation.* J Biol Chem, 2005. **280**(42): p. 35742-35750.
89. Metzger, M.B., Hristova, V.A., Weissman, A.M., *HECT and RING finger families of E3 ubiquitin ligases at a glance.* J Cell Sci, 2012. **125**: p. 531-537.
90. Glickman, M.H., Ciechanover, A., *The ubiquitin-proteasome proteolytic pathway: destruction for the sake of construction.* Physiol Rev., 2002. **82**(2): p. 373-428.
91. Thrower, J.S., Hoffman, L., Rechsteiner, M., Pickart, C.M., *Recognition of the polyubiquitin proteolytic signal.* EMBO J., 2000. **19**(1): p. 94-102.
92. Weissman, A.M., *Themes and variations on ubiquitylation.* Nat Rev Mol Cell Biol, 2001. **2**(3): p. 169-178.
93. Ardley, H.C., Robinson, P.A., *E3 ubiquitin ligases.* Essays Biochem., 2005. **41**(15-30).
94. Li, W., Bengston, M.H., Ulbrich, A., Matsuda, A., Reddy, V.A., Orth, A., Chanda, S.K., Batalov, S., Joazeiro, C.A., *Genome-wide and functional annotation of human E3 ubiquitin ligases identifies MULAN, a mitochondrial E3 that regulates the organelle's dynamics and signaling.* PLoS One, 2008. **3**(1): p. 1487.
95. Lorick, K.L., Jensen, J.P., Fang, S., Ong, A.M., Hatekeyama, S., Weissman, A.M., *RING fingers mediate ubiquitin-conjugating enzyme (E2)-dependent ubiquitination.* Proc Natl Acad Sci, 1999. **96**(20): p. 11364-11369.
96. Borden, K.L., Freemont, P.S., *The RING finger domain: a recent example of a sequence-structure family.* Curr Opin Struct Biol., 1996. **6**(3): p. 393-401.
97. Pickart, C.M., *Mechanisms underlying ubiquitination.* Annu Rev Biochem, 2001. **70**(503-533).
98. Neutzner, A., Li, S., Xu, S., Karbowski, M., *The ubiquitin/proteasome system-dependent control of mitochondrial steps in apoptosis.* Semin Cell Dev Biol, 2012. **23**(5): p. 499-508.

99. Oliner, J.D., Kinzler, K.W., Meltzer, P.S., George, D.L., Vogelstein, B., *Amplification of a gene encoding a p53-associated protein in human sarcomas.* Nature, 1992. **358**(6381): p. 80-83.
100. Finlay, C.A., *The mdm-2 oncogene can overcome wild-type p53 suppression of transformed cell growth.* Mol Cell Biol, 1993. **13**(1): p. 301-306.
101. Shadfan, M., Lopez-Pajares, V., Yuan, Z.M., *MDM2 and MDMX: Alone and together in regulation of p53.* Transl Cancer Res, 2012. **1**(2): p. 88-89.
102. Roy, N., Deveraux, Q.L., Takahashi, R., Salvesen, G.S., Reed, J.C., *The c-IAP-1 and c-IAP-2 proteins are direct inhibitors of specific caspases.* EMBO J., 1997. **16**(23): p. 6914-6925.
103. Duckett, C.S., Li, F., Wang, Y., Tomaselli, K.J., Thompson, C.B., Armstrong, R.C., *Human IAP-like protein regulates programmed cell death downstream of Bcl-xL and cytochrome c.* Mol Cell Biol, 1998. **18**(1): p. 608-615.
104. Benard, G., Neutzner, A., Peng, G., Wang, C., Livak, F., Youle, R.J., Karbowski, M., *IBRDC2, an IBR-type E3 ubiquitin ligase, is a regulatory factor for Bax and apoptosis activation.* EMBO J., 2010. **29**(8): p. 1458-1471.
105. Reddy, B.A., Etkin, L.D., Freemont, P.S., *A novel zinc finger coiled-coil domain in a family of nuclear proteins.* Trends Biochem Sci, 1992. **17**(344-345).
106. Borden, K.L., *RING fingers and B-boxes: zinc-binding protein-protein interaction domains.* Biochem Cell Biol, 1998. **76**(351-358).
107. Meroni, G., Diez-Roux, G., *TRIM/RBCC, a novel class of 'single protein RING finger' E3 ubiquitin ligases.* Bioessays, 2005. **27**(11): p. 1147-1157.
108. Torok, M., Etkin, L.D., *Two B or not two B? Overview of the rapidly expanding B-box family of proteins.* Differentiation, 2001. **67**(3): p. 63-71.
109. Urano, T., Saito, T., Tsukui, T., Fujita, M., Hosoi, T., Muramatsu, M., Ouchi, Y., Inoue, S., *Efp targets 14-3-3 sigma for proteolysis and promotes breast tumour growth.* Nature, 2002. **417**(6891): p. 871-875.
110. Dupont, S., Zacchigna, L., Cordenonsi, M., Soligo, S., Adorno, M., Rugge, M., Piccolo, S., *Germ-layer specification and control of cell growth by Ectodermin, a Smad4 ubiquitin ligase.* Cell, 2005. **121**(1): p. 87-99.
111. Niikura, T., Hashimoto, Y., Tajima, H., Ishizaka, M., Yamagishi, Y., Kawasumi, M., Nawa, M., Terashita, K., Aiso, S., Nishimoto, I., *Eur J Neurosci.* 17, 2003. **6**(1150-1158).
112. Reymond, A., Meroni, G., Fantozzi, A., Merla, G., Cairo, S., Luzi, L., Riganelli, D., Zanaria, E., Messali, S., Cainarca, S., Guffanti, A., Minucci, S., Pelicci, P.G., Ballabio, A., *The tripartite motif family identifies cell compartments.* EMBO J., 2001. **20**(9): p. 2140-2151.
113. Ogawa, S., Goto, W., Orimo, A., Hosoi, T., Ouchi, Y., Maramatsu, M., Inoue, S., *Molecular cloning of a novel RING finger-B box-coiled coil (RBCC) protein, terf, expressed in the testis.* Biochem Biophys Res Commun., 1998. **251**(2): p. 515-519.
114. Urano, T., Usui, T., Takeda, S., Ikeda, K., Okada, A., Ishida, Y., Iwanagi, T., Otomo, J., Ouchi, Y., Inoue, S., *TRIM44 interacts with and stabilizes terf, a*

TRIM ubiquitin E3 ligase. Biochem Biophys Res Commun., 2009. **383**(2): p. 263-268.
115. Desagher, S., Severac, D., Lipkin, A., Bernis, C., Ritchie, W., Le Digarcher, A., Journot, L., *Genes regulated in neurons undergoing transcription-dependent apoptosis belong to signaling pathways rather than the apoptotic machinery.* J Biol Chem, 2005. **280**(7): p. 5693-5702.
116. Miller, T.M., Tansey, M.G., Johnson, E.M., Creedon, D.J., *Inhibition of phosphatidylinositol 3-kinase activity blocks depolarization- and insulin-like growth factor I-mediated survival of cerebellar granule cells.* J Biol Chem, 1997. **272**(15): p. 9847-9853.
117. Cross, D.A., Culbert, A.A., Chalmers, K.A., Facci, L., Skaper, S.D., Reith, A.D., *Selective small-molecule inhibitors of glycogen synthase kinase-3 activity protect primary neurones from death.* J Neurochem., 2001. **77**(1): p. 94-102.
118. Lassot, I., Robbins, I., Kristiansen, M., Rahmeh, R., Jaudon, F., Magiera, M.M., Mora, S., Vanhille, L., Lipkin, A., Pettman, B., Ham, J., Desagher, S., *Trim17, a novel E3 ubiquitin-ligase, initiates neuronal apoptosis.* Cell Death and Differentiation, 2010. **17**(12): p. 1928-1941.
119. Endo, H., Ikeda, K., Urano, T., Horie-Inoue, K., Inoue, S., *Terf/TRIM17 stimulates degradation of kinetochore protein ZWINT and regulates cell proliferation.* J Biochem, 2012. **151**(2): p. 139-144.
120. Mattson, M.P., Gleichmann, M., Cheng, A., *Mitochondria in neuroplasticity and neurological disorders.* Neuron, 2008. **60**(5): p. 748-766.
121. Mattson, M.P., *Apoptosis in neurodegenerative disorders.* Nat Rev Mol Cell Biol, 2000. **1**(2): p. 120-129.
122. Dirnagl, U., Iadecola, C., Moskowitz, M.A., *Pathobiology of ischaemic stroke: an integrated view.* Trends Neurosci., 1999. **22**(9): p. 391-397.
123. Chan, S.L., Mattson, M.P., *Caspase and calpain substrates: roles in synaptic plasticity and cell death.* J Neurosci Res., 1999. **58**(1): p. 167-190.
124. Boya, P., Kroemer, G., *Lysosomal membrane permeabilization in cell death.* Oncogene, 2008. **27**(50): p. 6434-6451.
125. Franz, G., Beer, R., Intemann, D., Krajewski, S., Reed, J.C., Engelhardt, K., Pike, B.R., Hayes, R.L., Wang, K.K., Schutzhard, E., Kampfl, A., *Temporal and spatial profile of Bid cleavage after experimental traumatic brain injury.* J Cereb Blood Flow Metab., 2002. **22**(8): p. 951-958.
126. Plesnila, N., Zinkel, S., Le D.A., Amin-Hanjani, S., Wu, Y, Qiu, J., Chiarugi, A., Thomas, S.S., Kohane, D.S., Korsmeyer, S.J., Moskowitz, M.A., *BID mediates neuronal cell death after oxygen/ glucose deprivation and focal cerebral ischemia.* Proc Natl Acad Sci, 2001. **98**(26): p. 15318-15323.
127. Bermpohl, D., You, Z., Korsmeyer, S.J., Moskowitz, M.A., Whalen, M.J., *Traumatic brain injury in mice deficient in Bid: effects on histopathology and functional outcome.* J Cereb Blood Flow Metab., 2006. **26**(5): p. 625-633.
128. Yin, X.M., Luo, Y., Cao, G., Bai, L., Pei, W., Kuharsky, D.K., Chen, J., *Bid-mediated mitochondrial pathway is critical to ischemic neuronal apoptosis and focal cerebral ischemia.* J Biol Chem, 2002. **277**(44): p. 42074-42081.

129. Broughton, B.R., Reutens, D.C., Sobey, C.G., *Apoptotic mechanisms after cerebral ischemia.* Stroke, 2009. **40**(5): p. 331-339.
130. Hangen, E., Blomgren, K., Benit, P., Kroemer, G., Modjtahedi, N., *Life with or without AIF.* Trends Biochem Sci, 2010. **35**(5): p. 278-287.
131. Glassford, A., Lee, J.E., Xu, L., Giffard, R.G., *Caspase inhibitors reduce the apoptotic but not necrotic component of kainate injury in primary murine cortical neuronal cultures.* Neurol Res., 2002. **24**(8): p. 796-800.
132. Lang-Rollin, I.C.J., Rideout, H.J., Noticewala, M., Stefanis, L., *Mechanisms of Caspase-Independent Neuronal Death: Energy Depletion and Free Radical Generation.* J Neurosci, 2003. **23**(35): p. 11015-11025.
133. Becattini, B., Sareth, S., Zhai, D., Crowell, K.J., Leone, M., Reed, J.C., Pellecchia, M., *Targeting apoptosis via chemical design: inhibition of bid-induced cell death by small organic molecules.* Chem Biol., 2004. **11**(8): p. 1107-1117.
134. Ramonet, D., Perier, C., Recasens, A., Dehay, B., Bove, J., Costa, V., Scorrano, L., Vila, M., *Optic atrophy 1 mediates mitochondria remodeling and dopaminergic neurodegeneration linked to complex I deficiency.* Cell Death and Differentiation, 2012.
135. Krafft, P.R., Bailey, E.L., Lekic, T., Rolland, W.B., Altay, O., Tang, J., Wardlaw, J.M., Zhang, J.H., Sudlow, C.L., *Etiology of stroke and choice of models.* Int J Stroke., 2012. **7**(5): p. 398-406.
136. Venti, M., *Cerebellar infarcts and hemorrhages.* Front Neurol Neurosci., 2012. **30**(171-175).
137. Fortin, A., Cregan, S.P., MacLaurin, J.G., Kushwaha, N., Hickman, E.S., Thompson, C.S., Hakim, A., Albert, P.R., Cecconi, F., Helin, K., Park, D.S., Slack, R.S., *APAF1 is a key transcriptional target for p53 in the regulation of neuronal cell death.* J Cell Biol, 2001. **155**(2): p. 207-216.
138. Trempe, J.F., Chen, C.X., Grenier, K., Camacho, E.M., Kozlov, G., McPherson, P.S., Gehring, K., Fon, E.A., *SH3 domains from a subset of BAR proteins define a Ubl-binding domain and implicate parkin in synaptic ubiquitination.* Mol Cell, 2009. **36**(6): p. 1034-1047.
139. Ren, Y., Zhao, J., Feng, J., *Parkin binds to alpha/beta tubulin and increases their ubiquitination and degradation.* J Neurosci, 2003. **23**(8): p. 3316-3324.
140. Wilson, D.W., Whiteheart, S.W., Wiedmann, M., Brunner, M., Rothman, J.E., *A multisubunit particle implicated in membrane fusion.* J Cell Biol, 1992. **117**(3): p. 531-538.
141. Zhang, Q., Li, Y., Zhang, L., Yang, N. Meng, J., Zuo, P., Zhang, Y., Chen, J., Wang, L., Gao, Z., Zhu, D., *E3 ubiquitin ligase RNF13 involves spatial learning and assembly of the SNARE complex.* Cell Mol Life Sci., 2012.
142. Kar, N., Mishra, N., Singha, P.K., Venkatachalam, M.A., Saikumar, P., *Mitochondrial remodeling following fission inhibition by 15d-PGJ2 involves molecular changes in mitochondrial fusion protein OPA1.* Biochem Biophys Res Commun., 2010. **399**(4): p. 548-554.
143. Kim, W., Bennett, E.J., Huttlin, E.L., Guo, A., Li, J., Possemato, A., Sowa, M.E., Rad, R., Rush, J., Comb, M.J., Harper, J.W., Gygi, S.P., *Systematic*

and quantitative assessment of the ubiquitin-modified proteome. Mol Cell, 2011. **44**(2): p. 325-340.
144. Jahani-Asl, A., Pilon-Larose, K., William, X., MacLaurin, J.G., Park, D.S., McBride, H.M., Slack, R.S., *The mitochondrial inner membrane GTPase, optic atrophy 1 (Opa1), restores mitochondrial morphology and promotes neuronal survival following excitotoxicity.* J Biol Chem, 2011. **286**(6): p. 4772-4782.
145. Nijhawan, D., Fang, M., Traer, E., Zhong, Q., Gao, W., Du, F., Wang, X., *Elimination of Mcl-1 is required for the initiation of apoptosis following ultraviolet irradiation.* Genes Dev, 2003. **17**(12): p. 1475-1486.
146. Maurer, U., Charvet, C., Wagman, A.S., Dejardin, E., Green, D.R., *Glycogen synthase kinase-3 regulates mitochondrial outer membrane permeabilization and apoptosis by destabilization of MCL-1.* Mol Cell, 2006. **21**(6): p. 749-760.
147. Sitailo, L.A., Tibudan, S.S., Denning, M.F., *The protein kinase C delta catalytic fragment targets Mcl-1 for degradation to trigger apoptosis.* J Biol Chem, 2006. **2006**(281): p. 40.
148. Magiera, M.M., Mora, S., Mojsa, B., Robbins, I., Lassot, I., Desagher, S., *Trim17-mediated ubiquitination and degradation of Mcl-1 initiate apoptosis in neurons.* Cell Death and Differentiation, 2012.
149. Perciavalle, R.M., Stewart, D.P., Koss, B., Lynch, J., Milasta, S., Bathina, M., Temirov, J., Cleland, M.M., Pelletier, S., Schuetz, J.D., Youle, R.J., Green, D.R., Opferman, J.T., *Anti-apoptotic MCL-1 localizes to the mitochondrial matrix and couples mitochondrial fusion to respiration.* Nat Cell Biol, 2012. **14**(6): p. 575-583.
150. Sedlak, T.W., Oltvai, Z.N., Yang, E., Wang, K., Boise, L.H., Thompson, C.B., Korsmeyer, S.J., *Multiple Bcl-2 family members demonstrate selective dimerizations with Bax.* Proc Natl Acad Sci, 1995. **92**(17): p. 7834-7838.
151. Germain, M., Milburn, J., Duronio, V., *MCL-1 inhibits BAX in the absence of MCL-1/BAX Interaction.* J Biol Chem, 2008. **283**(10): p. 6384-6392.

Contribution of Collaborators

The YFP-Bax expressing Hela cells and the active Bax (6A7) antibody were a generous gift from Dr. David Andrews.

The Adenovirus expressing HA-tBid was a generous gift from Dr. Gordon Shore.

HEK293 Flp-In TRex cells and the pDest-FRT/TO and pOG44 vectors were a generous gift from Dr. Anne-Claude Gingras.

Darcey L. Miller carried out the two pilot screens for novel regulators of Bax activation.

Courtney Reeks performed the majority of the mouse dissections for cortical neurons and for whole brains. Darcey L. Miller performed some of the cortical neuron cell preparations.

The lab of Dr. Anne-Claude Gingras performed the FLAG-immunoprecipitation, in-gel extraction of silver-stained proteins and subsequent MS analysis for the two different proteomic screens.

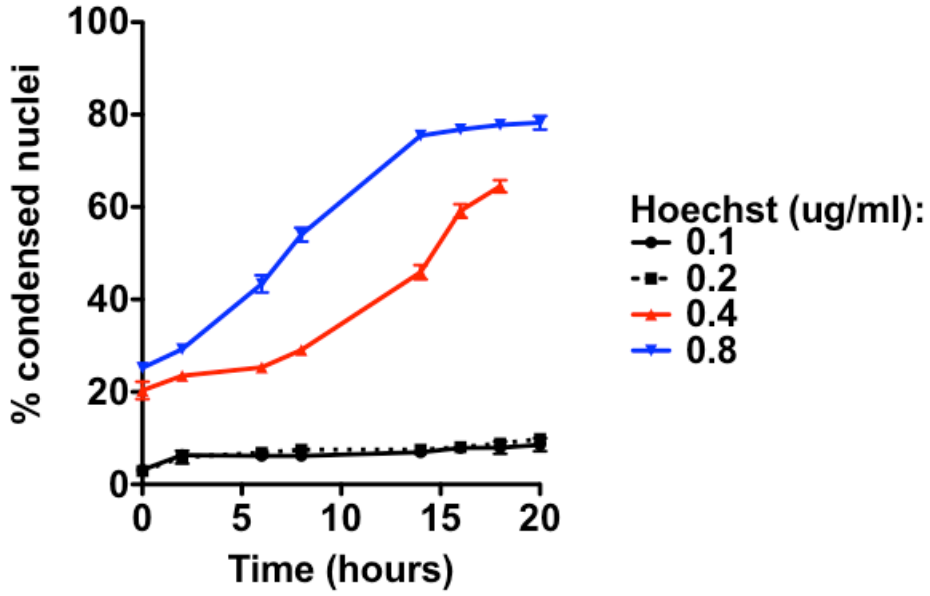

Appendix A. Verification of Hoechst toxicity in live cortical neurons for nuclear morphology assay. Live cells were incubated with various Hoechst concentrations and imaged over a 20 hr period. The number of condensed nuclei was quantified using an algorithm generated from the Columbus software (Perkin-Elmer). Hoechst concentrations < 0.2 ug/ml were found to be non-toxic over a 20 hr time course.

Appendix B. Mass spectrometry data for the top 98 hits from the HEK293 Flp-In Trex proteomic (I) screen. 3xFLAG-TRIM17 WT- or C16A-expressing cells were treated +/- etoposide prior to FLAG-IP and MudPIT mass spectrometry analysis. Tubulins were found to be top hit for both WT & C16A.

-

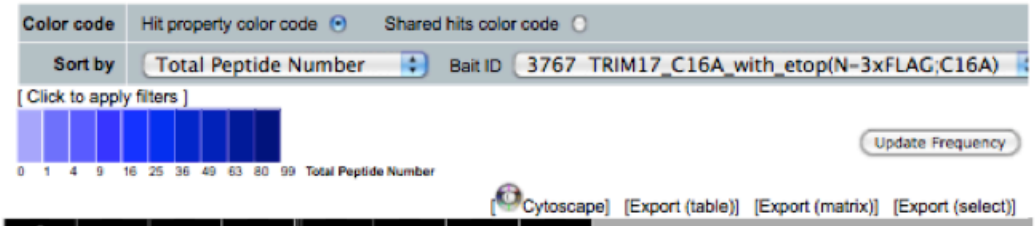

3767 TRIM17_C16A_with_etop(N-3xFLAG;C16A)	3766 TRIM17_C16A(N-3xFLAG;C16A)	3765 TRIM17_with_etop(N-3xFLAG)	3764 TRIM17(N-3xFLAG)	3763 Vector_with_etop_T	3762 Vector_no_etop_T	3759 Vector_with_etop_R	3758 Vector_no_etop_R	Hits		
								Gene Name	Protein ID	Peptide Comparison
76	69	99	79					TRIM17 [BioGRID]	7705825	
71						37		TUBA1B [BioGRID]	57013276	
71		71				35		TUBA1A [BioGRID]	17986283	
69	64	80	59	47	54	59	54	HSP90AA1 [BioGRID]	154146191	
69	78	80	68	35	44	40	36	TUBB [BioGRID]	29788785	
64	53	55	53	44	54	56	55	HSP90AB1 [BioGRID]	20149594	
63	67	74	58	33	45	40	37	TUBB2C [BioGRID]	5174735	
57	45	57	52	30	33	26	29	CCT2 [BioGRID]	5453603	
57	53	57	49		36	32		TUBB2B [BioGRID]	29788768	
57	52	55						TUBB2A [BioGRID]	4507729	
55	53	49	41	18	27	26	26	CCT8 [BioGRID]	48762932	
54	57	49	46	45	48	49	50	HSPA8 [BioGRID]	5729877	
48	52	43	40	42	37	37	45	HSPA1B [BioGRID]	167466173	
48	39	45	33				22	TUBA3E [BioGRID]	46409270	
47	56	61	50				27	TUBB4 [BioGRID]	21361322	
46	38	47	39	23	24	18	22	CCT3 [BioGRID]	63162572	
42	46	53	42	20	26	24	26	TCP1 [BioGRID]	57863257	
41	42	49	38	24	22	15	22	CCT5 [BioGRID]	24307939	
40	42	50	43	19	30	20	30	CCT4 [BioGRID]	38455427	
39			34					TUBB3 [BioGRID]	50592996	
38	28	16	17	24	30	36	40	MYH9 [BioGRID]	12667788	
38	28	28	29	30	36	42	52	FASN [BioGRID]	41872631	
38	38	33	30	12	23	18	23	CCT7 [BioGRID]	5453607	
36	44	40	48	30	52	46	48	FLNA [BioGRID]	116063573	
35	34	37	31	20	17	16	24	CCT6A [BioGRID]	4502643	
35	32	27	25	13	17	27	20	EIF4B [BioGRID]	50053795	
33	35	34	31				14	TUBB6 [BioGRID]	14210536	
32	42	26	31	18	28	26	31	PKM2 [BioGRID]	33286418	
30	32	36	32	35	31	35	34	FUS [BioGRID]	4826734	
26	32	28	24	22	19	22	26	GAPDH [BioGRID]	7669492	
24	20	11	10	24	25	29	29	IVNS1ABP [BioGRID]	24475847	
24	20	20	20	19	20	19	15	EEF1A1 [BioGRID]	4503471	
23	27	21	19	31	42	31	27	KIF11 [BioGRID]	13699824	

Appendix B. HEK293 Flp-In Trex proteomic screen (I) raw data (continued).

23	30	21	14	14	18	19	18	HSPA9 [BioGRID]	24234688	
23	21	16	16	20	19	22	27	STK38 [BioGRID]	6005814	
23	18	18	15	17	17	11	18	RPS3 [BioGRID]	15718687	
23	16	21	20	25	21	26	18	LUC7L2 [BioGRID]	116812577	
21	22	12	14	21	32	21	28	DDX46 [BioGRID]	41327773	
21	20	15	17	12	15	13	11	TRIM28 [BioGRID]	5032179	
21	17	14	16	9	16	16	18	SERBP1 [BioGRID]	66346683	
20	20	20	22	19	24	27	24	HSPA5 [BioGRID]	16507237	
20	20	24	28	18	24	18	25	VCP [BioGRID]	6005942	
20	23	18	18	20	21	18	24	HNRNPK [BioGRID]	14165435	
19	18	30	27	15	18	16	20	HSPD1 [BioGRID]	31542947	
19	17	18	15	17	19	25	20	ACTB [BioGRID]	4501885	
19	24	18	26	21	29	25	23	HSP90B1 [BioGRID]	4507677	
18	20	13	15	19	34	17	28	ACTN4 [BioGRID]	12025678	
18	13	12	10	16	13	13	14	LUC7L3 [BioGRID]	19923485	
18	11	15	12	17	18	14	12	PPM1B [BioGRID]	4505995	
17	23	16	12	11	11	12	14	STIP1 [BioGRID]	5803181	
17	11	7	9	15	20	21	22	PRPS2 [BioGRID]	4506129	
17			13		14		12	LUC7L [BioGRID]	8922297	
16	12	12	10	13	15	11	10	SUB1 [BioGRID]	217330646	
15	15	7	10	8	11	10	9	C1QBP [BioGRID]	4502491	
15	17	11	13	15	13	11	15	EIF3I [BioGRID]	4503513	
15	13	8	11	10	18	16	17	PRPS1 [BioGRID]	4506127	
14	16	21	19	5	16	7	3	VIM [BioGRID]	62414289	
14	8	8	13	3	6	10	12	CKB [BioGRID]	21536286	
14	13	15		7	15	5	5	KRT1 [BioGRID]	119395750	
14	8	14	13	5	8	9	9	DDX3X [BioGRID]	301171475	
14	11	11	11	11	14	16	12	YWHAE [BioGRID]	5803225	
14	14	14	18	17	17	18	16	HNRNPH1 [BioGRID]	5031753	
13	13	8	5	15	13	14	14	RIOK1 [BioGRID]	23510356	
13	18	15	11	2	1	2	3	DNAJA2 [BioGRID]	5031741	
13	13	13	14	13	12	16	15	ACTA1 [BioGRID]	4501881	
13	14	16	16	22	18	21	18	EWSR1 [BioGRID]	4885225	
13	9	8	5	4	10	9	9	PSMC4 [BioGRID]	5729991	
13	16	12	8	2		2		DNAJA1 [BioGRID]	4504511	
13	21	8	10	13	14	14	11	LSM14A [BioGRID]	166197710	
12	8	9	11	8	13	9	11	LRPPRC [BioGRID]	31621305	
12	9	4	2	3	2	2	3	SF3B3 [BioGRID]	54112121	
12	13	8	10	4	11	9	12	YBX1 [BioGRID]	34098946	
12	13	19	12	12	8	17	11	GTF2I [BioGRID]	14670350	
12	11	9	12	6	10	10	14	ALDOA [BioGRID]	4557305	
12	13	14	10	8	13	6	18	CLTC [BioGRID]	4758012	
12	6	9	6	5	7	9	6	YWHAB [BioGRID]	4507949	
12	10	8	13	12	20	16	16	RPL38 [BioGRID]	4506645	
11	9	7	3	13	11	17	15	PRPSAP2 [BioGRID]	4506133	
11	13	19	19	3	8	3	6	NCL [BioGRID]	55956788	
11	11	9	8	9	8	11	14	MYH10 [BioGRID]	41406064	
11	16	5	9	6	9	9	13	KPNB1 [BioGRID]	19923142	
11	10	14	10	15	15	7	14	BCLAF1 [BioGRID]	7661958	
11	7	12	14	6	15	12	9	XRCC5 [BioGRID]	10863945	
11	8	11	9	1	8	6	7	RPS4X [BioGRID]	4506725	
11	11	13	10	10	22	18	17	THRAP3 [BioGRID]	167234419	
11				5				KRT2 [BioGRID]	47132620	
11	9	5	8	8	15	12	11	EIF3G [BioGRID]	49472822	
10	9	9	9	10	16	8	11	RBM10 [BioGRID]	20127479	
10	10	5	4	7	7	11	14	MTHFD1 [BioGRID]	222136639	
10				14	19	11	17	ACTN1 [BioGRID]	194097350	
10	12	11	12	9	10	8	11	CLNS1A [BioGRID]	4502891	
10	2	5	4	4	3	6	5	PSMD1 [BioGRID]	25777600	
10	13	11	12	14	14	11	15	CIRBP [BioGRID]	4502847	
10	6	8	5	8	9	6	6	RPS14 [BioGRID]	5032051	
10	6	2	3	9	7	9	8	EPPK1 [BioGRID]	207452735	
10	12	7	11	11	11	6	8	PIN4 [BioGRID]	38579892	
9	12	5	2	3	6	7	8	PSMD3 [BioGRID]	25777612	
9	14	8	9	12	9	19	14	ENO1 [BioGRID]	4503571	

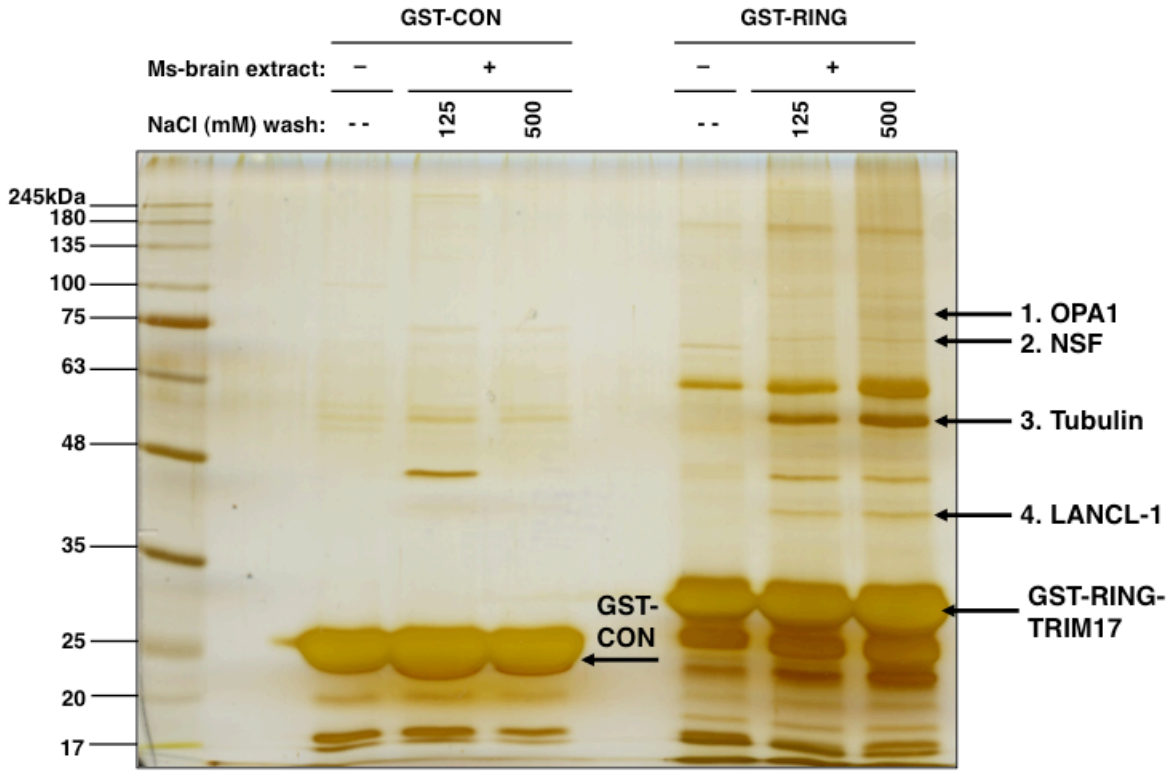

Appendix C. Proteomic screen (II) to identify interacting partners of the RING domain of TRIM17. Silver-stained gel showing pulldown of potential interacting partners from mouse brain extracts using GST-CONTROL or GST-RING-TRIM17 bait. Bands unique to TRIM17 are marked with arrows. The bands were analyzed by mass spectrometry and identified to be (1) OPA1, (2) NSF, (3) tubulin & (4) LANCL-1.

Band	Gene Name	Gene ID	Protein ID	Total Peptide Number
1	**Opa1**	**74143**	**19526960**	**32**
	Prss1	114228	16716569	17
	Hsp90aa1	15519	6754254	12
	Gpc1	14733	7710028	10
	Hsp90ab1	15516	40556608	10
	Ddx1	104721	19527256	8
	Tuba1a	22142	6755901	7
	Hnrnpul1	232989	21450323	6
	Nrxn1	18189	226958325	6
	Psmd2	21762	19882201	5
	Spock2	94214	16506279	5
	Gstm1	14862	6754084	5
	Dgkg	110197	20149724	5
	Dhx15	13204	110835723	5
	Spock1	20745	50053938	5
	Lingo1	235402	30841016	4
	Vwa5a	67776	225543183	3
	Kpnb1	16211	88014720	3
	Gstm5	14866	6754086	3
	Sv2a	64051	11528518	3
	Dclk2	70762	40254281	3
	Mars	216443	51491852	3
	Copg2	54160	8567340	2
	Atp2a2	11938	6806903	2
	Canx	12330	6671664	2
	Efr3b	668212	126723102	2
	Ntrk2	18212	6679150	2
	Sirpa	19261	110626109	2
2	**Nsf**	**18195**	**31543349**	**72**
	Ppm1g	14208	6679793	28
	Hspa5	14828	254540166	20
	Hspa12a	73442	28461135	19
	Syn1	20964	160707901	16
	Acsl6	216739	75992911	15
	Try10	436522	84781771	15
	Ncl	17975	84875537	12
	Ncdn	26562	172072590	11
	Adam23	23792	6752968	9
	Ddx3x	13205	6753620	6
	Marcks	17118	6678768	6
	Hadha	97212	33859811	4
	Mccc1	72039	186700620	3
	Crtac1	72832	110626040	3
	Ngef	53972	162417957	3
	Tubb5	22154	7106439	2
	Jup	16480	28395018	2
	Srp72	66661	118344452	2
	Gstp1	14870	10092608	2

Band	Gene Name	Gene ID	Protein ID	Total Peptide Number
4	**Lancl1**	**14768**	**21489937**	**67**
	Idh3a	67834	18250284	13
	Gnao1	14681	6754012	8
	Idh3b	170718	18700024	5
	Tuba1c	22146	6678469	5
	Gnai2	14678	41054806	4
	Gnai1	14677	74271899	4
	Idh3g	15929	6680345	4
	Got2	14719	6754036	3
	Dsp	109620	82950149	3
	Bccip	66165	134031957	3
	Acta2	11475	6671507	2
	Anxa2	12306	6996913	2
	Mapt	17762	84370347	2
	Gnaz	14687	27532946	2
	Hdac11	232232	21450317	2

Appendix D. Mass spectrometry data for bands 1 (~90kDa), 2 (~74kDa) and 4 (~40kDa) from pulldown with GST-RING-TRIM17 in mouse brain extracts.

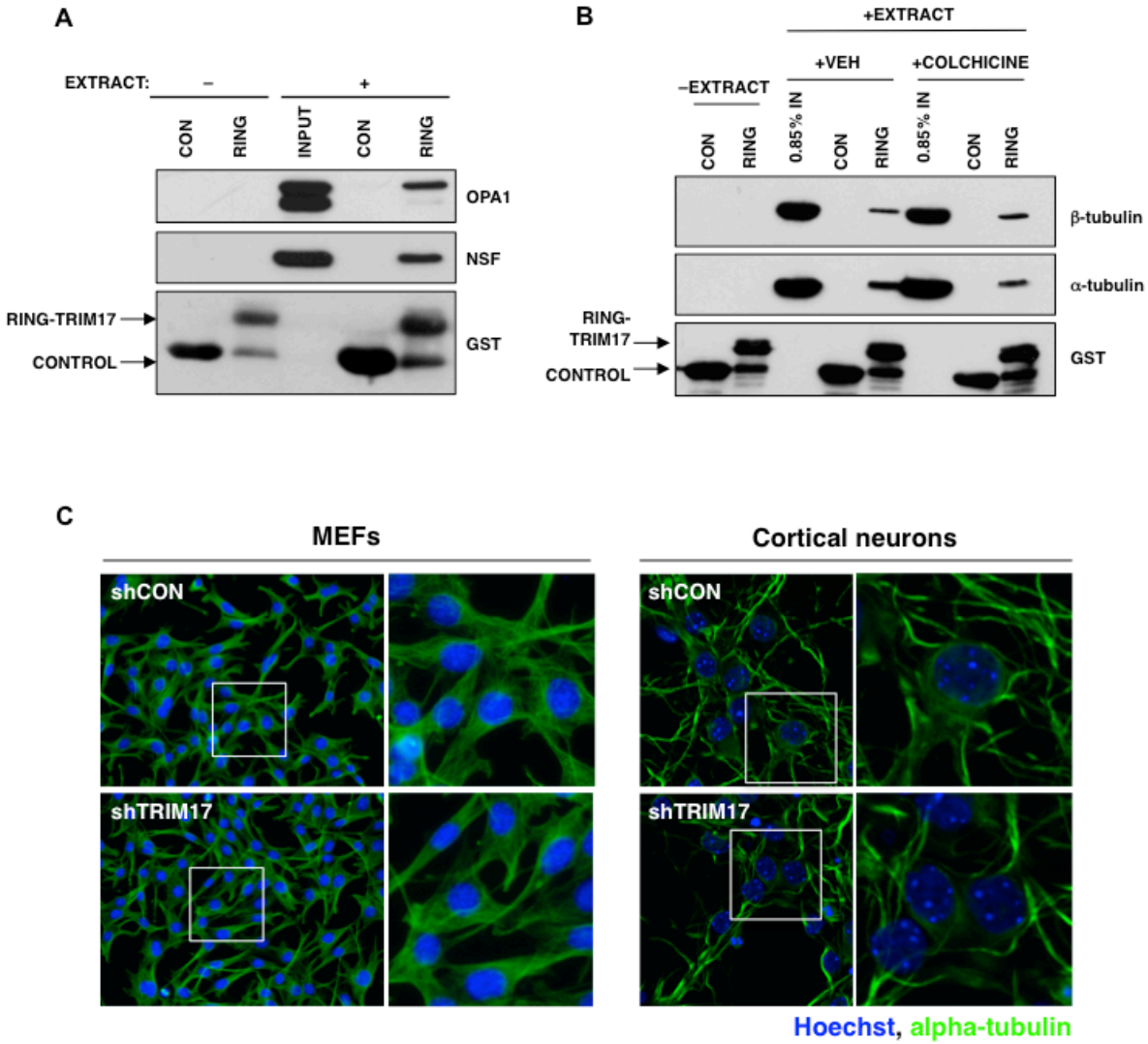

Appendix E. The RING domain of TRIM17 forms a complex with NSF and both alpha- and beta-tubulin in mouse brain extracts. A. Western blot showing pulldown of NSF with specifically with GST-RING-TRIM17. B. Western blot showing pulldown of both tubulin forms with GST-RING-TRIM17. This interaction was not disrupted by the microtubule destabilizer colchicine. B. Loss of Trim17 does not affect steady-state alpha-tubulin morphology in MEFs and in cortical neurons. Immunofluorescence images showing that alpha-tubulin morphology is the same in control and Trim17 knockdown cells.

Curriculum Vitae

Education

September 2010 – present	MSc Biochemistry, University of Ottawa
September 2005 – December 2009	BSc, major in Biochemistry, Carleton University

Research Experience

September 2010 – September 2012	MSc research student, Apoptosis Research Centre, Children's Hospital of Eastern Ontario Research Institute, Ottawa, Ontario
November 2008 – August 2009	Honours research student, Department of Chemistry, Carleton University, Ottawa, Ontario

Awards and Honours

September 2011 – August 2012	Ontario Graduate Scholarship
September 2010 – August 2012	Ontario Graduate Scholarship in Science and Technology
September 2010 – August 2012	University of Ottawa Excellence Scholarship
September 2007 – April 2009	Deans' Honour List for Academic Achievement (Carleton University)
September 2005 – April 2009	Canadian Interuniversity Sport Academic-All Canadian
September 2008 – April 2009	Carleton University Entrance Scholarship
September 2005 – April 2006	Carleton University Entrance Scholarship

Graduate Classes Completed

BCH8105	Advanced Topics in the Molecular Biology of Human Diseases (A+)
BCH8106	Advanced Topics in Nutrition and Regulation of Metabolism (A+)
BCH5366	MSc Seminar

Presentations

October 2011	Cold Spring Harbor Meeting on Cell Death – Poster Presentation
October 2011	4th Annual Children's Hospital of Eastern Ontario Research Day – Poster presentation

Publications

Kong, H.I., Crichton, J.E., Manthorpe, J.M. (2011). *Stereoselective synthesis of ambiphilic alkenes via regioselective methylation of α-trifluoromethanesulfonyl carbonyl compounds with trimethylsilyldiazomethane.* Tetrahedron Letters, 52(29): 3714–3717